LBL-13562
Preprint

Lawrence Berkeley Laboratory

UNIVERSITY OF CALIFORNIA

RECEIVED
LAWRENCE
BERKELEY LABORATORY
DEC 1 1981
LIBRARY AND
DOCUMENTS SECTION

Materials & Molecular Research Division

Submitted to Nuclear Engineering and Design

VAPMIG - A MODEL OF BRINE MIGRATION AND WATER TRANSPORT IN ROCK SALT SUPPORTING A TEMPERATURE GRADIENT

D.R. Olander

November 1981

TWO-WEEK LOAN COPY

This is a Library Circulating Copy which may be borrowed for two weeks. For a personal retention copy, call Tech. Info. Division, Ext. 6782

Prepared for the U.S. Department of Energy under Contract W-7405-ENG-48

LBL-13562 c.2

DISCLAIMER

This document was prepared as an account of work sponsored by the United States Government. While this document is believed to contain correct information, neither the United States Government nor any agency thereof, nor the Regents of the University of California, nor any of their employees, makes any warranty, express or implied, or assumes any legal responsibility for the accuracy, completeness, or usefulness of any information, apparatus, product, or process disclosed, or represents that its use would not infringe privately owned rights. Reference herein to any specific commercial product, process, or service by its trade name, trademark, manufacturer, or otherwise, does not necessarily constitute or imply its endorsement, recommendation, or favoring by the United States Government or any agency thereof, or the Regents of the University of California. The views and opinions of authors expressed herein do not necessarily state or reflect those of the United States Government or any agency thereof or the Regents of the University of California.

LBL-13562

VAPMIG - A Model of Brine Migration and Water Transport in Rock Salt Supporting a Temperature Gradient

D. R. Olander

Materials and Molecular Research
Division of the Lawrence Berkeley
Laboratory and the
Department of Nuclear Engineering
University of California
Berkeley, California 94720

This work was supported by the Director, Office of Energy Research, Office of Basic Energy Sciences, Materials Sciences Division of the U.S. Department of Energy under contract # W-7405-ENG-48.

ABSTRACT

A computer code VAPMIG which combines brine inclusion migration and vapor transport by Knudsen and bulk diffusion in interconnected porosity has been developed to predict the release of water and brine to a drillhole in rocksalt which is heated by nuclear waste. Inclusions move under the influence of the temperature gradient only as far as the boundary of the grain they are in. At the grain boundary the migrating inclusions are trapped and deliver their brine and volume to the interconnected porosity. Further transport of water occurs via the vapor phase. The salt porosity near the drillhole is assumed to be increased by the boring operation. During nuclear heating, the porosity can change because of the trapping of inclusions from within the salt crystals and by thermomechanical effects (thermal and lithostatic stresses and creep consolidation). This effect is modeled by simple closure due to thermal expansion. A base-case calculation and sensitivity analyses are performed with the code. The most important parameters affecting water release are: the extent of porosity closure by thermomechanical effects (this phenomenon can also cause extrusion of liquid brine at the drillhole surface); the permeability of the salt to gas; and the fraction of the intra- and intergranular brine which communicates with the interconnected porosity. Judicious choice of the parameters produces water release rates which are comparable to those observed in field tests.

I. INTRODUCTION

In anticipation of application for a license from the Nuclear Regulatory Commission, the Department of Energy has sought to establish the technical performance of repositories for disposal of high level nuclear wastes in geologic salt formations. A significant issue in this technical evaluation is the behavior of the water contained in natural salt when the latter is subjected to the thermal nonuniformity created by emplacement of the heat-generating waste canisters. This phenomenon has been treated in detail in a comprehensive review by Jenks and Claiborne(1). The object of the analysis of water in salt is to predict the amount of water and/or brine which will be transported to the drillhole containing the nuclear wasteform during the latter's lifetime.

There is no disputing that water in rocksalt is mobilized by application of a temperature gradient. Intragranular brine inclusions move by a solution-diffusion mechanism driven by the temperature dependence of the salt solubility and by the Soret effect. Intergranular water, on the other hand, can escape by vapor transport or by flow as a liquid along the microcracks and grain boundaries which are rendered permeable by the mechanical action of boring the drillhole (and the consequent release of the lithostatic pressure on the salt) and by the thermal stresses and creep due to the temperature gradient. Transport models have been developed for both of these mechanisms, each to the exclusion of the other.

The MIGRAIN code(2) considers only migration of brine inclusions

within crystalline salt; it computes the total water inflow to the drillhole by assuming that inclusions migrate as entities until they reach the canister surface. Grain boundaries are ignored in this treatment.

In the model proposed by Hadley and Faris(3), all water is transported as a vapor through grain boundary channels. Motion of the intragranular brine inclusions is not permitted; instead, these act as reservoirs of water which are made available to the vapor transport process only as the receding vapor-liquid interface passes them.

The neglect of interaction between migrating inclusions and grain boundaries of rock salt is a fatal shortcoming of the MIGRAIN approach. A number of investigations have shown that except for very "tight" boundaries such as can be fabricated by joining two single crystals, inclusions driven by the thermal gradient do not penetrate the boundary. On the other hand, the Hadley-Faris model provides no description of the kinetics of the process by which water in inclusions reaches grain boundaries where it becomes available for release. In addition, the inclusions bring their volume as well as their brine when they reach a grain boundary, and the former property serves to increase the porosity of the grain boundaries which govern water release by vapor transport. The VAPMIG model described in this report attempts to weld these two approaches into a consistent framework which includes all pertinent physical processes affecting water mobility in nonisothermal rocksalt.

II THE DRYING MODEL

The model assumes an infinitely long drillhole of radius R_o in an infinite extent of rocksalt (axial end effects are not considered). The drillhole at all times is flushed with dry air at 1 bar pressure. The

total water content of rocksalt varies from that characteristic of dome salt ($\sim$ 0.02 volume percent) to that of bedded salt (up to 1%). This native water in the original salt is divided into two parts:

ϕ^{o}_{gb} = initial volume fraction of brine present on grain boundaries

ϕ_{incl} = initial volume fraction of brine as intragranular inclusions

It is assumed that the act of drilling the hole in the salt increases the porosity of the solid, either by opening up existing grain boundaries or by creating new microfissures in the grains. This mechanically-induced porosity is described by the two-parameter function:

$$\frac{\phi_{gb} - \phi^{o}_{gb}}{\phi_{gbo} - \phi^{o}_{gb}} = \exp[-g(\eta - 1)] \qquad (1)$$

where:

$$\eta = r/R_o \qquad (2)$$

is the radial position measured in units of drillhole radii.

The porosity produced by drilling and by relief of the lithostatic stress will undoubtedly be largest at the surface of the drillhole, where its value is denoted by ϕ_{gbo}. The recovery of the porosity of the virgin salt is assumed to be exponential in distance from the drillhole with the rapidity of decay of the porosity governed by the dimensionless parameter g. The porosity described by Eq(1) is assumed to be interconnected and to lead to the drillhole surface so that it provides a pathway for water vapor or brine to escape from the salt. Equation(1) describes the interconnected porosity of the salt before the temperature field due to the wasteform is imposed upon the solid. During the period of nuclear

heating, the porosity function changes due to a number of processes which will be detailed later.

The quantity ϕ°_{gb} represents only that part of the native grain boundary brine which is part of the interconnected porosity. There may be additional liquid in closed intergranular pores. As long as these pores do not move and do not become linked to the open porosity, they play no role in the water release process.

During application of the temperature field, the quantity of water in the open porosity is given by the function:

$C(\eta,t)$ = volume fraction of brine present in the open porosity at radial location η and time t

Since the quantity of intergranular brine cannot exceed the volume available to accommodate it,

$$C \lesssim \phi_{gb} \tag{3}$$

To simulate the construction and loading schedule of an actual repository, a delay of a year or so is assumed between the digging of the drillhole and the emplacement of nuclear waste in the hole. During this period, the open porosity is assumed to be maintained at the radial distribution given by Eq(1); no creep consolidation is permitted. During the initial isothermal drying period, water is lost from the hole by vapor transport from a receding interface. The transport process is assumed to be a combination of Knudsen and bulk diffusion. Hydrodynamic (D'Arcy) flow is neglected. No other process acts to change the intergranular water content, which is therefore given by:

$$C(\eta,t) = \begin{cases} 0 & \text{if } 1 \leq \eta \leq \eta_L \\ \phi^{\circ}_{gb} & \text{if } \eta_L \leq \eta \end{cases}$$

where η_L is the time-dependent interface location. The brine in the connected porosity during the isothermal period is shown schematically in Fig. 1. If the interface location is η_L, the zone $1 \leq \eta \leq \eta_L$ contains no liquid. In the region $\eta > \eta_L$, the brine does not fill the available porosity. No vapor transport occurs in the two-phase zone because it is isothermal. Liquid redistribution by capillarity is not considered. The intragranular inclusions are immobile during this period.

At a time denoted by $t = 0$, the nuclear waste is placed in the hole. The time-dependent temperature distributions which result from this heat source are calculated by a heat conduction code. For this purpose, the distributions given by Ref. 4 have been used. The temperature rise accelerates loss of water by vapor transport in the open porosity but it also mobilizes the intragranular brine which has been dormant during the preceding isothermal drying period. In addition, thermal expansion of the salt acts to reduce the open porosity. Finally, establishment of a temperature gradient in the zone of partially-liquid-filled porosity causes water vapor transport down the temperature gradient. Thus, water is transported by diffusion away from the vapor-liquid interface in <u>both</u> directions.

The inclusions are assumed to migrate in the thermal gradient at a velocity given the Jenks formula(1). The rate at which inclusions reach the boundary of the grain that contains them depends upon the radial location (which determines the temperature and temperature gradient) and

the size of the salt grain. In accord with the observation of Roedder and Belkin(5), inclusions which reach a grain boundary are assumed to lose their identity and to deliver their brine and volume to the grain boundary. The smaller gas-liquid inclusions which are spawned by this interaction and which migrate back down the temperature gradient(5) are neglected. Only a fraction of this liquid source is deposited in the connected porosity. The remainder becomes attached to portions of grain boundary of microcracks which do not communicate with the network of open porosity. These inclusions are effectively trapped or immobilized and cannot contribute to water migration to the drillhole. Thus the term ϕ_{incl} is interpreted as the actual volume fraction of intragranular brine multiplied by the fraction which, upon reaching a grain boundary, contributes to the open porosity. This class of brine eventually escapes to the drillhole by vapor transport.

Mineralogical examination of the sides of the drillhole in the Salt Block II experiment(6) revealed efflorescences which were interpreted as the residue of liquid brine had escaped from the salt during the test and evaporated to dryness on the cavity wall. This phenomenon can occur if the open porosity is reduced by thermomechanical effects (i.e. the thermal expansion or creep) more rapidly than it is increased by arrival of inclusions from the grains or if the rate of brine supply from the grain interior exceeds the loss rate by vapor transport to the drillhole. For these cases, the liquid front in the porous solid advances rather than recedes and can reach the drillhole surface where liquid spills out. If thermomechanical pore closure is not considered, all water loss occurs by vapor transport.

The following sections present the equations governing the component

steps in the overall water loss process.

III TRANSPORT OF WATER VAPOR

A. The Flux Equations

As in Ref. 3, movement of gaseous water in the porous salt is assumed to take place by a combination of Knudsen and bulk diffusion in the air/water mixture. Hydrodynamic(D'Arcy) flow is neglected because of the presumed small characteristic dimensions of the pores and the modest pressures involved. The rates of the diffusional transport processes are linear in the pressure gradient whereas hydrodynamic flow depends upon the gradient of the square of the pressure.

The basic diffusive flux equations in a porous medium are given by Gunn and King(7). In applying these equations to water movement in porous salt, quasi-steady state can be assumed and the flux of the air component set equal to zero. At radial location r the water vapor flux in the radial direction, N_w, expressed in gram moles per unit area of the porous solid is:

$$N_w = - \frac{c_2 D^* K_w}{RT(PK_w + c_2 D^*)} \frac{dp_w}{dr} + \frac{p_w K_w}{(PK_w + c_2 D^*)} N_w \qquad (4)$$

where P is the total gas pressure and p_w is the partial pressure of water; both are functions of radial position. R is the gas constant and T the temperature. D* is the product of the mutual diffusion coefficient of the air-water mixture and the total pressure. The parameter c_2 depends only on the structure of the porous medium and represents the ratio of the bulk

diffusivity in the porous solid to the free gas bulk diffusivity. The Knudsen diffusivity of water vapor in the porous solid is related to another constant characterized by the pore structure, c_1, by:

$$K_w = c_1 (RT/M_w)^{\frac{1}{2}} \tag{5}$$

where M_w is the molecular weight of water.

The corresponding flux equation for air is:

$$0 = - \frac{c_2 D^* K_a}{RT(PK_a + c_2 D^*)} \frac{dp_a}{dr} + \frac{p_a K_a}{(PK_a + c_2 D^*)} N_w \tag{6}$$

where K_a is the Knudsen diffusion coefficient of air in the porous salt. It is given by Eq(5) with M_w replaced by the molecular weight of air. The partial pressure of air in the pores, p_a, is related to the total pressure and the water vapor pressure by:

$$P = p_a + p_w \tag{7}$$

The gas transport properties of the salt are characterized by the two structure-sensitive constants, c_1 and c_2; however, in the present analysis it is convenient to replace the former by K_w according to Eq(5) and the latter by the dimensionless parameter:

$$A = \frac{p_{ao} K_w}{c_2 D^*} \tag{8}$$

where p_{ao} is the partial pressure of air in the drillhole.

As shown by Gunn and King(7), the water flux N_w can be eliminated from Eqs(4) and (6) and the resulting equation integrated from the drillhole

surface ($r = R_o$) to obtain the following relation between the partial pressures of the two components:

$$1 - \xi - \frac{\ln\xi}{A} = y - y_o \tag{9}$$

where

$$\begin{aligned} \xi &= p_a/p_{ao} \\ y &= p_w/p_{ao} \end{aligned} \tag{10}$$

and y_o is the ratio of the partial pressures of water and air in the drillhole. The water flux is determined from Eqs(4) and (7) as:

$$N_w = -\frac{\left(\frac{K_w}{RT}\right)}{1+A\xi}\frac{dp_w}{dr} = -\frac{\left(\frac{K_w p_{ao}}{RTR_o}\right)}{1+A\xi}\frac{dy}{d\eta} \tag{11}$$

The limit as $A \to 0$ corresponds to dominance of Knudsen diffusion and the water vapor flux reduces to:

$$(N_w)_{Knudsen} = -\left(\frac{K_w}{RT}\right)\frac{dp_w}{dr} \tag{12}$$

As $A \to \infty$, the solution of Eq(9) is $\xi = 1+y_o-y$ and Eq(11) reduces to the formula for ordinary diffusion of one component in a stagnant gas. In general, Eq(9) must be solved for ξ as a function of y and substituted into Eq(11).

B. Salt Permeability

In addition to creation of microfissures, the permeability induced in the salt by digging the hole for the waste canister is probably due to opening up of existing grain boundaries. In the latter case, the porosity consists of thin sheets surrounding the grains. The porosity

increase is due to enlargement of the grain boundary width δ, or $\delta \propto \phi_{gb}$. The free-molecule conductance of thin annular or rectangular slots varies as the square of the slot width(8), or $K_w \propto \delta^2$. Thus, if porosity distributions such as that given by Eq(1) are due to separation of existing grain boundaries in the salt, the Knudsen permeability varies with radius according to:

$$K_w = K_{wo}(\phi_{gb}/\phi_{gbo})^2 \tag{13a}$$

where K_{wo} is the Knudsen diffusivity which characterizes the initial permeability of the salt immediately adjacent to the drill hole. During the initial isothermal drying period, the porosity ratio in the above formula is given by Eq(1). Thermal effects on the porosity during the subsequent heating phase are reflected in the permeability distribution via Eq(13).

If the predominant effect of drillhole boring and lithostatic stress relief is creation of microcracks in the grains rather than opening of grain boundaries, both the porosity and the permeability depend on the crack density (assuming that all cracks are of the same size). In this case the permeability distribution would be:

$$K_w = K_{wo}(\phi_{gb}/\phi_{gbo}) \tag{13b}$$

In general, a mixture of grain boundary separation and microcracking leads to a permeability distribution in the salt which varies as the porosity distribution raised to a power between one and two. In the absence of data which would permit distinction between these two possibilities, the grain boundary separation model of Eq(13a) has been used in the calculations.

The remaining structural permeability parameter, c_2, is assumed to vary with porosity in the same manner as does K_w, so that the parameter A of Eq(8) is a constant.

C. Isothermal Drying Period

Water removal during the period between drillhole boring and emplacement of nuclear waste in the hole is treated by classical drying theory. The water flux of Eq(11) is integrated and combined with a water balance on the system. The rate of water loss from the salt per unit length of drillhole surface, q, is related to the water flux in the porous salt by:

$$q = -2\pi r N_w = q_o \frac{\eta(\phi_{gb}/\phi^\circ_{gb})^2}{1+A\xi} \frac{dy}{d\eta} \tag{14}$$

The second equality in this equation was obtained by expressing the water flux N_w by Eq(11). The quantity q_o is defined by:

$$q_o = \frac{2\pi K_{wo}\, p_{ao}}{RT(\phi_{gbo}/\phi^\circ_{gb})^2} \tag{15}$$

Integration of Eq(14) between the drillhole surface and the vapor-liquid interface gives:

$$q \int_1^{\eta_L} \frac{d\eta}{\eta(\phi_{gb}/\phi^\circ_{gb})^2} = q_o \int_{y_o}^{y_L} \frac{dy}{1+A\xi}$$

where

$$y_L = p_w^{sat}/p_{ao} \tag{16}$$

and p_w^{sat} is the vapor pressure of water in equilibrium with saturated brine at the system temperature. By changing the variable of integration on the right hand side of the above equation from y to δ by use of

Eq(9), the integral can be analytically evaluated. The rate of water loss becomes:

$$q = q_o\left(\frac{-\ln\xi_L}{A}\right)\Bigg/\int_1^{\eta_L} \frac{d\eta}{\eta(\phi_{gb}/\phi^\circ_{gb})^2} \tag{17}$$

where ξ_L is the relative pressure of air at the vapor liquid interface, which is obtained by solution of Eq(9) with $y = y_L$. The porosity ratio in the integral is given by Eq(1). To determine the position of the interface, the water balance on the dry zone in Fig. 1 gives:

$$q = 2\pi R_L \phi^\circ_{gb}\ \rho_w \frac{dR_L}{dt} = \tau_o\ \eta_L \frac{d\eta_L}{dt} \tag{18}$$

where R_L is the radial location of the vapor-liquid interface and ρ_w is the molar density of water in saturated brine at the temperature of the isothermal drying period. The parameter τ_o is given by:

$$\tau_o = 2\pi R_o^2 \phi^\circ_{gb}\ \rho_w \tag{19}$$

As discussed at the beginning of Section II, the intergranular water content of the brine-containing zones ($\eta > \eta_L$ in Fig. 1) is equal to ϕ°_{gb} during the isothermal drying period. Equating the right hand sides of Eqs(17) and (18) and integrating for the duration t_{iso} of the isothermal drying period during which the vapor-liquid interface recedes from $\eta_L = 1$ to $\eta_L = \eta_{L0}$ yields:

$$\int_1^{\eta_{L0}} \eta_L d\eta_L \int_1^{\eta_L} \frac{d\eta}{\eta(\phi_{gb}/\phi^\circ_{gb})^2} = \frac{q_o}{\tau_o}\left(\frac{-\ln\xi_L}{A}\right) t_{iso} \tag{20}$$

For a specified isothermal drying period, Eq(20) determines the position of the vapor-liquid interface at the time of introduction of the nuclear waste into the drillhole.

D. Intragranular Brine Flow to the Grain Boundaries

During the isothermal drying period analyzed in the preceding section, the brine inclusions inside the salt crystals do not move because no temperature gradient is present. Introduction of the heat source into the hole sets up temperature nonuniformities which cause the intragranular brine to move radially inwards. During a time measured from the end of the isothermal drying period, all inclusions which reach the boundary of the grain in which they are located cease to exist and contribute their brine and their volume to the interconnected porosity. The kinetics of this process depend upon the inclusion migration velocity and the grain size. A closely related process occurs in nuclear fuels containing fission gas bubbles, in which the grain boundaries collect gas reaching the boundaries from the interior by bubble migration(9). In both cases, the process can be analyzed by assuming spherical grains of diameter d_g containing an initially uniform distribution of inclusions. At $t = 0$, the inclusions acquire mobility denoted by the velocity V, which is radially directed and which has the same magnitude for all inclusions. If the inclusions were not impeded by the grain boundary, the sphere of inclusions after time t would be displaced as shown in Fig. 2. However, the grain boundary traps all inclusions reaching it, and the ratio of such inclusions to those in the original sphere is equal to the ratio of the shaded volume in Fig. 2 to the sphere volume. The sphere displacement is measured by the quantity h, which is defined by $dh/dt = -V$. From the solid geometry of the intersecting spheres in Fig. 2, the fraction of

inclusions reaching the grain boundary is(9):

$$f = 1 - \frac{1}{2}H^2(3-H) \tag{21}$$

where:

$$H = \frac{h}{d_g} = 1 - \frac{1}{d_g}\int_0^t V(\eta,t')dt' \tag{22}$$

The inclusion velocities (in cm/yr) are given by the Jenks Equation(1):

$$\log(V/\nabla T) = 0.00656T - 0.6036 \tag{23}$$

Where T is the temperature in °C and ∇T is the local temperature gradient in °C/cm.

The quantity of water in the inclusions contained in a unit volume of salt is $\rho_w\phi_{incl}$ and a fraction f of this water is deposited on the grain boundaries in time t. The source term representing the rate of water supply to the grain boundaries by inclusion migration per unit volume of salt is:

$$S = \frac{d}{dt}(\rho_w\phi_{incl}f) = \rho_w\phi_{incl}\frac{df}{dt}$$

From Eq(21):

$$\frac{df}{dt} = (-3H + \frac{3}{2}H^2)\ \frac{dH}{dt} = (3H - \frac{3}{2}H^2)\ \frac{V}{d_g}$$

so that the rate of supply of water to the connected porosity from inclusions reaching the grain boundaries is:

$$S = \frac{\rho_w\phi_{incl}}{d_g}(3H - \frac{3}{2}H^2)V(\eta,t)$$

or:

$$S = \frac{\tau_o}{2\pi R_o^2} \left(\frac{\phi_{incl}}{\phi^o_{gb}}\right) (3H - \tfrac{3}{2}H^2) \quad \frac{V(\eta,t)}{d_g} \tag{24}$$

where τ_o is given by Eq(19).

For a specified time-dependent temperature distribution, $V(\eta,t)$ is determined by Eq(23), $H(\eta,t)$ by Eq(22), and $S(\eta,t)$ follows from Eq(24).

E. Water Loss by Vapor Transport

In the dry zone shown in Fig. 1, all water in the connected porosity is assumed to be present as vapor. The supply from inclusions given by Eq(24) is assumed to vaporize as soon as the brine-filled cavities empty their contents into the grain boundary. The water balance on the vapor in the dry zone is:

$$\frac{1}{r}\frac{d}{dr}(rN_w) = S(r,t) \tag{25}$$

Converting to the dimensionless radial position variable and integrating yields:

$$\eta N_w - N_w(\eta=1) = R_o \int_1^{\eta} \eta' S(\eta',t)d\eta' \tag{26}$$

The rate at which water enters the drillhole per unit height is:

$$q = -\ 2\pi R_o N_w(\eta=1)$$

Eliminating $N_w(\eta=1)$ by the above equation and N_w by Eq(11), Eq(26) becomes:

$$q = q_o \frac{(\phi_{gb}/\phi^o_{gb})^2}{1 + A\xi} \frac{dy}{d\eta} + 2\pi R_o^2 \int_1^{\eta} \eta' S(\eta',t)d\eta'$$

where Eq(13a) has been used. Multiplying this equation by $d\eta$ and integraing over the range $1 \leq \eta \leq \eta_L$ results in:

$$q = \frac{q_o\left(\frac{-\ln\xi_L}{A}\right) + 2\pi R_o^2 \int_1^{\eta_L} \frac{d\eta}{\eta(\phi_{gb}/\phi^\circ_{gb})^2} \int_1^{\eta} \eta' S(\eta',t)d\eta'}{\int_1^{\eta_L} \frac{d\eta}{\eta(\phi_{gb}/\phi^\circ_{gb})^2}} \tag{27}$$

In the absence of inclusion motion ($S = 0$), Eq(27) reduces to Eq(17) which was derived for the isothermal drying period.

F. Brine Content of the Two-Phase Zone

No brine is present in the dry zone and the region labeled "filled pores" in Fig. 1 contains no vapor. The volume fraction of brine in the open porosity in these two zones is given by:

$$C(\eta,t) = 0 \qquad \text{for } 1 \leq \eta \leq \eta_L$$

$$C(\eta,t) = \phi_{gb} \qquad \text{for } \eta > \eta^*$$

In the intermediate two-phase zone, the volume fraction of brine is determined by a water balance. There are two sources of water in an element of volume in the two-phase region. The first and most important is the source from the intragranular inclusions derived in Section IIID. The other is water transport by diffusion in the gas space not occupied by liquid in this zone; because a temperature gradient is impressed on the solid and the local partial pressure of water in the two-phase zone is equal to the saturation pressure, a water pressure gradient must

exist and lead to diffusion of water radially outward. Denoting this flux by N_w' the water balance in the two-phase region is given by:

$$\rho_w \left(\frac{dC}{dt}\right)_{sources} = S - \frac{1}{r} \frac{d}{dr} (rN_w')$$

In addition to the sources of water, the volume fraction of brine increases with time because of thermal expansion. This process is described by:

$$\left(\frac{dC}{dt}\right)_{exp} = \alpha_B C \frac{\partial T}{\partial t}$$

where α_B is the coefficient of thermal expansion of brine. Adding these two components of dC/dt yields:

$$\frac{d(C/\phi^\circ_{gb})}{dt} = \frac{2\pi R_o^2}{\tau_o} S - \frac{2\pi R_o}{\tau_o} \frac{1}{\eta} \frac{d}{d\eta} (\eta N_w') + \alpha_B \left(\frac{C}{\phi^\circ_{gb}}\right) \frac{\partial T}{\partial t} \tag{28}$$

The initial condition for this equation is:

$$C/\phi^\circ_{gb} = 1 \text{ at } t = 0 \text{ for all } \eta > \eta_{L0}$$

The vapor flux N_w' in the two-phase region is of the same form as that in the dry zone given by Eq(11). However, because the partial pressure of water in the pores is assumed to be equal to the saturation pressure at the local temperature,

$$\frac{dy}{d\eta} = \frac{1}{p_{ao}} \frac{dp_w^{sat}}{d\eta} = \frac{1}{p_{ao}} \frac{dp_w^{sat}}{dT} \frac{dT}{d\eta} \tag{29}$$

In addition, the vapor space available for diffusion is reduced by the presence of brine in the pores, so that instead of Eq(13a), K_w is given by:

$$K_w = K_{wo} \left(\frac{\phi_{gb} - C}{\phi_{gbo}} \right)^2 \tag{30}$$

Substituting these equations into the water flux expression of Eq(11) yields:

$$N'_w = \frac{\frac{q_o}{2\pi R_o} \left(\frac{\phi_{gb}}{\phi^o_{gb}} - \frac{C}{\phi^o_{gb}} \right)^2 \frac{1}{p_{ao}} \frac{dp_w^{sat}}{dT} \frac{dT}{d\eta}}{1 + A\xi} \tag{31}$$

The bulk diffusion correction factor in the denominator is given by modifying Eq(9) to apply to the two-phase zone:

$$\xi_L - \xi - \frac{\ln(\xi/\xi_L)}{A} = y - y_L \tag{32}$$

where $y = p_w^{sat}/p_{ao}$ and y_L is the value of this ratio at the vapor-liquid interface ($\eta = \eta_L$). The quantity ξ_L is the ratio of the partial pressure of air at the interface to p_{ao}, and is obtained from Eq(9) with y replaced by y_L.

G. Porosity Changes

The porosity associated with grain boundaries or microcracks affects both the permeability of the salt (via Eqs(13a) or (13b)) and the capacity of the solid to store intergranular water. The latter property is important; should the porosity decrease, the brine contained in it could

be extruded from the salt like toothpaste from a tube.

The time rate of change of the intergranular porosity at each radial location in the solid can be broken down into three components. The first is the increase due to arrival at the grain boundary of inclusions from within the grains. The second is a decrease due to precipitation of salt as a consequence of evaporation of water from the brine in the dry zone or an increase because of water addition to the brine in the two-phase zone. The third component, which may either increase or decrease porosity, is due to thermomechanical effects such as thermal expansion or creep consolidation. Both of these phenomena are dependent on the local stresses in the salt. The creep closure effect is related to the healing of cracks in ceramic nuclear fuels. The local porosity variation with time can be written as:

$$\frac{\partial \phi_{gb}}{\partial t} = \left(\frac{\partial \phi_{gb}}{\partial t}\right)_{incl} + \left(\frac{\partial \phi_{gb}}{\partial t}\right)_{evap} + \left(\frac{\partial \phi_{gb}}{\partial t}\right)_{\substack{thermo-\\mech}} \tag{33}$$

Each of the components on the right hand side of this equation is treated below:

1. <u>Inclusions</u>

Equation(24) gives the number of moles per second of liquid water which arrive as brine at the grain boundaries in a unit volume of salt. Division of this quantity by the number of moles of water per unit volume of brine yields the volume source term:

$$\left(\frac{\partial \phi_{gb}}{\partial t}\right)_{incl} = \frac{S}{\rho_w} = \frac{2\pi R_o^2 \phi_{gb}^{\circ} S}{\tau_o} \tag{34}$$

This term is identical to the first term on the right hand side of Eq.(28)

because the volume of brine and the volume of the cavity of an all-liquid intragranular inclusion are equal.

2. Evaporation

Salt precipitation (which reduces porosity) occurs in the dry zone because the inclusions reaching the grain boundaries are assumed to evaporate to dryness. If ρ_s^{sat} moles salt/cm^3 brine is the concentration of dissolved salts (including impurities such as Mg^{2+}) in the inclusions and d_s moles salt/cm^3 solid is the density of the precipitate remaining when all water evaporates, the volume of precipitated solid is equal to the fraction ρ_s^{sat}/d_s of the original brine volume. Thus:

$$\left(\frac{\partial\phi_{gb}}{\partial t}\right)_{evap} = -\frac{\rho_s^{sat}}{d_s}\left(\frac{\partial\phi_{gb}}{\partial t}\right)_{incl} \quad \text{for } 1 \lesssim \eta \lesssim \eta_L \tag{35}$$

In the two-phase zone of Fig. 1, the water flux N_w' is directed radially outward and decreases with increasing distance from the drillhole. Therefore, the water vapor transport process in this zone tends to dilute the brine. Since the system acts to restore saturated conditions, solid salt dissolves and the porosity increases. The component of the porosity change due to evaporative transfer at radial positions in this zone can be written as:

$$\left(\frac{\partial\phi_{gb}}{\partial t}\right)_{evap} = \frac{\partial\phi_{gb}}{\partial C}\left(\frac{\partial C}{\partial t}\right)_{evap}$$

where $\partial\phi_{gb}/\partial C$ is the increase in porosity per unit increase in brine volume due to addition of pure water provided by condensation of water vapor. This term is equal to ρ_s^{sat}/d_s. Strictly speaking, the densities in this ratio are not the same as those in the comparable ratio in Eq(35) because

the latter applies to intragranular inclusions which contain alkaline earth ions not present in the halite. However, this distinction is ignored in the present analysis. The second term in the above equation is equal to the second term on the right hand side of Eq(28); thus the porosity rate of change due to vapor transport of water in the two-phase region of salt interconnected porosity is:

$$\left(\frac{\partial \phi_{gb}}{\partial t}\right)_{evap} = - \frac{\rho_s^{sat}}{d_s} \frac{2\pi R_o \phi_{gb}^{o}}{\tau_o} \frac{1}{\eta} \frac{d}{d\eta} (\eta N_w') \text{ for } \eta_L \leq \eta \leq \eta^* \qquad (36)$$

No evaporation or condensation of water vapor occurs in the brine-filled zone at $\eta > \eta^*$.

3. Thermomechanical Effects

The rise in salt temperature upon introducing nuclear waste into the drillhole establishes compressive thermal stresses in the salt which act to reduce intergranular porosity. The reverse effect, that due to cooling, is to enlarge the pores and/or to create new cracks. The effect of temperature reduction on the permeability and hence on the water release rate was dramatically demonstrated in the Project Salt Vault and the Salt Block II experiments(1). However, the effects of salt cooling are of no consequence in repository design because essentially all brine inflow is expected to occur while the temperatures in the vicinity of the drillhole are still increasing. In contrast to an electrically heated experiment, it is impossible to abruptly lose nuclear heat.

Enhanced water release on heating was observed in the Salt Block II tests(10). Whether these increases were due to a thermal stress-induced porosity increase or simply to increase of the vapor pressure of water in

the salt at the elevated temperatures is not known. There is evidence(11) that the porosity of small salt specimens is increased by isothermal heating. However, in a repository, particularly if the drillhole is lined with a metal sleeve, increasing temperatures will most likely lead to porosity reduction and reduced water permeability. The extent of the reduction is a function of stress and the compressibility of the grain boundaries. Hadley and Faris(3) assumed that the porosity depends only on the residual strain obtained directly from the stress analysis (the residual strain is the total strain from which the thermal expansion strain has been deducted). No account was taken of the strain response of the grain boundaries or microcracks to the applied stresses; the pertinent properties needed for such an analysis are not available. Finally, the interconnected porosity will change with time under constant stress because of creep of the salt. At the present time, there is no known method of accounting for this phenomenon.

In the present analysis, the grain boundary porosity changes are assumed to be a specified fraction F of the thermal expansion of the salt:

$$\left(\frac{\partial \phi_{gb}}{\partial t}\right)_{\substack{\text{thermo-}\\ \text{mech.}}} = - F\left(\frac{1}{3}\alpha_s\right)\frac{\partial T}{\partial t} \qquad (37)$$

where α_s is the volume expansion coefficient of solid salt. The factor $\frac{1}{3}$ appears because the porosity is slab-like, so volume changes occur only by alteration of the width of the grain boundaries. The fraction F is intended to represent the degree of constraint of the salt in the repository design. If no sleeve lines the drillhole, the salt can expand thermally into the drillhole

rather than close internal porosity; in this case, $F \to 0$. At the other extreme, salt heated in a rigid container must expand thermally into all internal void spaces; for this limit, $F \to 1$.

Substitution of Eqs(34), (35) or (36), and (37) into Eq(33) produces the total time rate of change of the interconnected porosity. The initial condition for its integration is the porosity distribution given by Eq(1).

H. Location of the Vapor-Liquid Interface

The last step in the analysis is determination of the interface position η_L as a function of time by a total water balance on the salt. During the isothermal drying period the required water balance is simple and leads directly to the differential equation given by Eq(18). In the heating phase, however, the inclusions add water to the interconnected porosity, vapor transport occurs in the two-phase zone, and the open porosity changes with time. These complications are best dealt with by a water balance expressed in integral rather than differential form.

Water is conserved out to $\sim$ 10 drillhole radii in the salt. This cutoff is designated as η_{max} in Fig. 1. Beyond this position, all water motion is arbitrarily zero. At the start of the heating period, the water contained in a unit height of salt is:

$$\text{initial water} = \pi(R_{max}^2 - R_o^2)\phi_{incl}\,\rho_w + \pi(R_{max}^2 - R_{L0}^2)\phi_{gb}^{\circ}\rho_w$$

The first term on the right hand side of this equation is the original water content of the inclusion, which do not move under isothermal conditions. At the end of the isothermal drying period, the vapor-liquid interface is at radial location R_{L0} which is determined by

solving Eq(20). The original intergranular water in the salt is present at larger radii.

After time t of heating, the water in the salt is:

$$\text{water at time } t = 2\pi\rho_w \int_{R_L}^{R_{max}} rC(r,t)dr + 2\pi\rho_w\phi_{incl} \int_{R_o}^{R_{max}} r[1-f(r,t)]dr$$

The first term represents water in the open porosity and the second term is water in the brine inclusions which remain in the salt crystals.

The difference between the above water contents is the cumulative release, whether as water vapor:

$$Q_v = \int_0^t q dt' \tag{38}$$

or as liquid, Q_ℓ. In terms of the dimensionless radial position, the water balance is:

$$\frac{1}{2}(\eta_{max}^2 - \eta_{L0}^2) - \frac{Q_v + Q_\ell}{\tau_o} + \left(\frac{\phi_{incl}}{\phi_{gb}^o}\right)\int_1^{\eta_{max}} \eta f(\eta,t)\, d\eta = \int_{\eta_L}^{\eta_{max}} \eta\left(\frac{C}{\phi_{gb}^o}\right)d\eta \tag{39}$$

The unknown interface position appears as the lower limit in the integral on the right hand side of this equation. During the isothermal drying period, $f = 0$, $Q = 0$, $C/\phi_{gb}^o = 1$ and the derivative of Eq(39) with respect to time yields Eq(18).

IV COMPUTER PROGRAM DESCRIPTION

The calculations described in Sect. III are organized into the computer code VAPMIG in the manner shown in the flow chart of Fig. 3. Input information is shown in ovals and calculational procedures in rectangles. Conditions for a spent fuel repository were taken from Ref. 4. The drillhole radius is 30.5 cm and the waste is a 10-yr-old spent fuel assembly. The temperature distributions for times up to ten years after insertion of the waste into the hole are shown in Fig. 4.

For computing efficiency, the functions describing intragranular brine release to the grain boundaries [$f(\eta,t)$ and $S(\eta,t)$ of Sect. IIID] and their integrals [the S-integral in Eq(27) and the f-integral in Eq(39)] are computed only once and stored for use in subsequent calculations. The inclusion velocity function and the size of the salt crystals are used only in this step. Doubling the grain size has the same effect as halving the inclusion velocity.

Time steps of 0.05 to 0.2 years are sufficiently small to produce reliable results. At the start of a new time step, the vapor flux in the two-phase zone (if one exists) is calculated from the previous profiles of ϕ_{gb} and C by use of Eq(31). This calculation is needed only in the range $\eta_L \lesssim \eta \lesssim \eta^*$, for which the limits at the previous time are used.

Next the new porosity distribution is computed from the previous one by time-stepping of Eq(33), using Eqs(34), (35) or (36), and (37) for the computation of $\Delta\phi_{gb}$.

Then the change in the intergranular brine fraction, ΔC, is computed from Eq(28) for all radii > η_L. The calculation is stopped at the location η^* where C becomes equal to ϕ_{gb}. Thereafter the pores are full of brine.

After computing the increment in the cumulative vapor loss during the time step, the position of the vapor-liquid interface is determined from Eq(39). At this point in the program, the entire left-hand side of this equation and the intergranular brine profile $C(\eta,t)$ are known for the current time. The integral on the right-hand side of Eq(39) is performed from the upper limit backwards in space; the position at which the integral on the right becomes equal to the left-hand side of the equation defines the new value of the interface position, η_L. If the integration is carried to $\eta = 1$ and the right hand side of Eq(39) is still less than the left-hand side, then the cumulative brine loss to the drillhole, Q_ℓ, is increased to achieve closure of the water balance.

Finally the vapor release rate q at the current time is calculated from Eq(27) and the entire process repeated for the next time step.

The input parameters needed to perform the calculation (in addition to the temperature distributions) are listed in Table 1. A base-case calculation utilizing the numerical values given in the next-to-last column was performed. Since many of the parameters in the table are either poorly known or totally unknown, sensitivity calculations were also performed. These consisted of changing one parameter at a time of the base case set. The parameter changes for the sensitivity calculations are given in the last column of Table 1.

RESULTS AND DISCUSSION

Various aspects of the base-case calculation are shown in Figs. 5 and 6. The isothermal drying period was 0.44 yrs, at which time the vapor-liquid interface position (η_{L0}) was 1.5, or $\sim$ 15 cm from the edge of the drillhole. During the heating phase, the calculated position at the interface increased continually, reaching η_L = 7 drillhole radii after 7 years. The outer limit of the two-phase zone increased from η^* = 10 at the start of heating and joined the η_L (interface) curve after 3 years. Thereafter, the brine zone in the open porosity remained full of liquid.

The cumulative vapor loss is low at the beginning of the transient but accelerates after $\sim$ ½ year. Increased vapor escape is calculated (despite recession of the interface) because of the increasing temperature at the vapor-liquid interface. This temperature rise provides driving forces which are more than sufficient to make up for the longer diffusional transport paths due to interface recession.

The combination of the Jenks inclusion velocity equation, the temperature gradients in Fig. 4, and the 0.5 cm diameter grain size produce very significant losses of inclusion brine from the crystals. At the end of 4 years of heating, the salt grains out to 2.5 drillhole radii have lost all of their intragranular water. Even as far out as 10 drillhole radii, the grains are > 50% depleted of brine. This easily releasable water source is in large part responsible for the substantial cumulative vapor releases shown in Fig. 5. The cumulative value of $\sim$ 8 moles/cm after 7 years, for example, corresponds to $\sim$ 30 liters of water collected from a 2 m deep hole.

Figure 6 shows profiles of the open porosity and the grain boundary brine content for several times during the transient. The porosity is seen to increase regularly with time at all radial positions. This behavior is due to the volume increase caused by arrival of inclusions at the grain boundaries. Between 5 and 10 years, no further porosity changes occur close to the surface because all of the intragranular brine has been driven from the salt earlier in the heat treatment.

Figure 7 shows the sensitivity of the calculation to the Knudsen-to-bulk diffusion coefficient ratio (i.e., the parameter A of Eq(8)). Increasing A from 10^{-2} to 1 while keeping K_{wo} constant is equivalent to introducing a bulk diffusion resistance of comparable magnitude to the Knudsen diffusion resistance. As seen in Fig. 7, the release rate decreases relative to the base case and the interface recedes more slowly.

Figure 8 shows the effect of an initial mechanically-induced porosity at the surface of the drillhole (ϕ_{gbo}) which is only 25% greater than the original porosity ϕ°_{gb} instead of 100% larger as in the base case. Compared to the base case results in Fig. 5, the reduction of initial porosity has a relatively small effect on water loss rates. The reason for this is that the intergranular porosity becomes enlarged by migration of inclusions to the grain boundaries, thereby eliminating the effect of the initially more constricted pore structure.

The effect of the depth of penetration into the solid of the initial porosity change, as measured by the parameter g, is shown in Fig. 9. The more extensive porosity implied by g = 0.5 instead of g = 1.0 leads to somewhat higher release rates. However, as the case

of decreasing ϕ_{gbo} discussed above, the increase in initial porosity and its depth of penetration into the salt is greatly mitigated by the porosity developed by the capture of migrating inclusions at grain boundaries.

Elimination of all intragranular porosity ($\phi_{incl} = 0$) produces the curves shown in Fig. 10. The halving of the cumulative water loss compared to the base case is simply a result of the fact that salt contains half as much water as it did in the base case calculation. In addition, expansion of the porosity on the grain boundaries by inclusions is absent, so vapor transport is more restricted than in the base case.

The grain size has only a minor effect on water loss. Figure 11 shows that increasing the grain size from 0.5 to 1.0 cm decreases the cumulative water loss by only $\sim$ 10%. This decrease is due to the slower rate of supply of intragranular water to the grain boundaries in the large-grained salt compared to that in the salt with the smaller grains.

The base case and the single-parameter changes discussed above were all based on the assumed absence of thermomechanical effects on the open porosity (i.e., the parameter F in Eq(37) was zero). The effects of allowing 50% of the thermal expansion of the solid salt to be accommodated by the grain boundary porosity are shown in Figs. 12 and 13. The latter plot shows that the porosity of the salt at first decreases (because of thermal expansion of the solid) and after $\sim$ 1 year increases as the migrating inclusion begin to reach the grain boundaries in significant numbers. By contrast, in the base case, the porosity at the grain boundaries increased monotonically with time (Fig. 6). As shown in Fig. 12, the initial porosity decrease causes the vapor-liquid interface

to advance from its initial location rather than to retreat into the solid. Very shortly after start of the heating, the interface has reached the drillhole surface. This extrusion effect dominates for the first 3 months of operation and during this period a sizeable quantity of liquid brine flows into the drillhole. This mechanism may have been the reason for the observation of efflorescences on the walls of the Salt Block II experimental specimen(6). After $\sim$ 6 months, vapor transport re-establishes the normal drying behavior and the interface recedes slowly into the salt.

Except for thermomechanical closure of intergranular porosity, none of the parameters of the model discussed above have a drastic effect on the water release rate. However, the two remaining parameters, namely the salt permeability reflected in the Knudsen diffusivity K_{wo} and the fraction of the included water which is active in the release process, are quite significant.

The brine available for release in the base case was set equal to 0.1%, equally divided between inter- and intragranular components. This water content lies between those found in typical dome and bedded salts. The model assumes that all of this brine takes part in the release process, which is responsible for the calculated release of over 50% of all of the water in the salt out to 10 drillhole radii in 7 years. Experience with water release in Project Salt Vault and the Salt Block II experiment indicates that this degree of brine availability is too high. To simulate the inaccessibility of most of the inter- and intragranular brine to the release mechanisms, the effective initial grain boundary porosity ϕ^{o}_{gb} was reduced by a factor of 10. The initial intragranular brine fraction, ϕ_{incl}, was reduced by the same fraction. This means that 90% of the brine in the salt is either trapped in closed grain boundary pores or, if free

to migrate intragranularly as inclusions, arrives at portions of grain boundaries which do not communicate with the open porosity.

In addition, an experimentally-based Knudsen diffusion coefficient was used in place of the arbitrarily-selected value of 10^4 cm^2/yr used in the base-case calculation. Jenks and Claiborne(1) report of a measurement of the D'Arcy permeability to nitrogen measured within the first 4 cm of a drillhole in the Avery Island salt dome. According to D'Arcy's law, the flux of gas is related to the permeability κ by:

$$N = - \frac{P\kappa}{RT\mu} \frac{\partial P}{\partial r}$$

where μ is the gas viscosity. If the permeability is in fact due to Knudsen flow rather than to hydrodynamic flow, the appropriate flux law is Eq(12). Therefore, the D'Arcy permeability can be converted to a Knudsen permeability by:

$$K = \frac{P\kappa}{\mu}$$

Assuming P = 1 bar in the Avery Island tests, μ = 175 micropoises for nitrogen and using the experimentally determined permeability of 3 fcm^2 yields a Knudsen diffusivity of 500 cm^2/yr from the above formula.

The predicted cumulative water release for the smaller values of ϕ°_{gb} and K_{wo} discussed above are shown in Fig. 14. The cumulative release at the end of 7 years is 0.5 moles/cm, or for a heated length of 2 m, a volume of water equal to 1.8 liters. The experimental points for water collected in the Project Salt Vault and the Salt Block II experiment, also shown in Fig. 14, are higher than the calculated curve. This

discrepancy is in the right direction because the experimental points reflect significant releases due to accidental cooling events during the tests. This type of anomoly is not considered in the theoretical model.

VI CONCLUSIONS

A procedure for calculating the loss of water as vapor or as brine in a borehole containing nuclear waste has been developed. The method accounts for vapor transport of water by Knudsen and bulk diffusion in the open porosity of the salt and brine movement by inclusion migration in the salt crystals and by extrusion from the interconnected porosity. Aside from the temperature distribution, the parameters which have the most profound effect on the water loss are the salt permeability, the closure of interconnected porosity by thermal expansion or stress, and the fraction of the grain boundary porosity, whether originally in the salt or created by trapped intragranular inclusions, which is interconnected and provides a fluid pathway to the drillhole. Reasonable estimates of the parameters of the model produces water release predictions which are consistent with field tests in rock salt.

VII ACKNOWLEDGMENT

This work was supported by the Director, Office of Energy Research, Office of Basic Energy Sciences, Materials Sciences Division of the U.S. Department of Energy under contract # W-7405-ENG-48.

REFERENCES

1. G. H. Jenks and H. C. Claiborne, "Brine Migration in Salt and Its Implications in the Geologic Disposal of Nuclear Waste", Draft Topical Technical Report for ONWI, July 1981.
2. H. C. Claiborne, L. D. Rickertsen and R. F. Graham, "Expected Envirnoments in High-Level Nuclear Waste and Spent Fuel Repositories in Salt", ORNL/TM - 7201, August 1980.
3. G. R. Hadley and G. W. Faris, "Revised Theory of Water Transport in Rock Salt", SAND 80-2398 (1980).
4. H. Waldman, "Evaluation of the Thermomechanical Behavior of a Waste Container/Sleeve in Salt", ONWI - 235 (1981).
5. E. Roedder and H. E. Belkin, "Migration of Fluid Inclusions in Polycrystalline Salt under Thermal Gradients in the Laboratory and in Salt Block II", in Proc. of the 1980 National Waste Terminal Storage Program Information Meeting, ONWI-212, p. 361 (1980).
6. S. J. Lambert, "Mineralogical Aspects of Fluid Migration in the Salt Block II Experiment", SAND 79 - 2423 (1979).
7. R. D. Gunn and C. J. King, "Mass Transport in Porous Materials under Combined Gradients of Composition and Pressure", AIChE J., 15 507 (1969).
8. C. M. Van Atta, "Vacuum Science and Engineering", p 61, McGraw-Hill (1965).
9. J. R. Matthews and M. H. Wood, "Modeling the Transient Behavior of Fission Gas", J. Nucl. Mater. 84, 125 (1979).
10. G. R. Hadley, "Salt Block II: Brine Migration Modeling", SAND 81 - 0438 (1981).

11. F. M. Sears, "Analysis of Microcracks in Dry Polycrystalline NaCl by Ultrasonic Signal Processing", UCRL-52975 (1980).

FIGURE CAPTIONS

Figure 1. Brine distribution in porous rock salt surrounding heat-generating nuclear waste canister.

Figure 2. Movement of inclusions in a spherical grain due to a temperature gradient. Those inclusions in the shaded portion of the displaced sphere are trapped by the grain boundary.

Figure 3. Flow diagram of the computer code VAPMIG.

Figure 4. Temperature distributions around the drillhole at various times after emplacement of nuclear waste (from Ref. 4).

Figure 5. Location of brine-vapor interfaces and cumulative vapor outflow during drying of rock salt by nuclear waste heating. The base-case conditions used for the calculation are given in Table 1.

Figure 6. Porosity and brine distributions for the base-case calculation at various times following emplacement of nuclear waste in the drillhole.

Figure 7. Effect of the relative importance of Knudsen and bulk diffusion on salt drying characteristics: The base case parameters except for A, which has been changed from 0.01 to 1.

Figure 8. Effect on salt drying of the initial porosity increase at the drillhole surface: base-case parameters except for ϕ°_{gb}, which was decreased from $2\phi^{\circ}_{gb}$ to $1.25\ \phi^{\circ}_{gb}$.

Figure 9. Effect on salt drying of the extent of the porosity increase due to drillhole boring: the base-case parameters except for g, which was changed from 1.0 to 0.5.

Figure 10. Effect of intragranular brine content on salt drying: base case parameters except for ϕ_{incl}, which has been set equal to zero.

Figure 11. Effect of grain size on the water loss rate from heated rock salt: base case parameters except for d_g, which was increased from 0.5 cm to 1.0 cm.

Figure 12. Effect on salt drying of pore closure by thermal expansion: base case parameters except for F, which was changed from 0 to 0.5.

Figure 13. Porosity closure during heating and water removal from rock salt: base case parameters except for the thermal expansion parameter F, which was increased from 0 to 0.5.

Figure 14. Drying of salt using the best estimate transport and structural parameters: base case conditions except for K_{wo}, which was reduced from 10^4 cm^2/yr to 500 cm^2/yr, and the fraction of the brine which is available for release, which was decreased from 100% to 10%. The cumulative releases in two large-scale field tests are shown for comparison with the theoretical curve labelled Q_v.

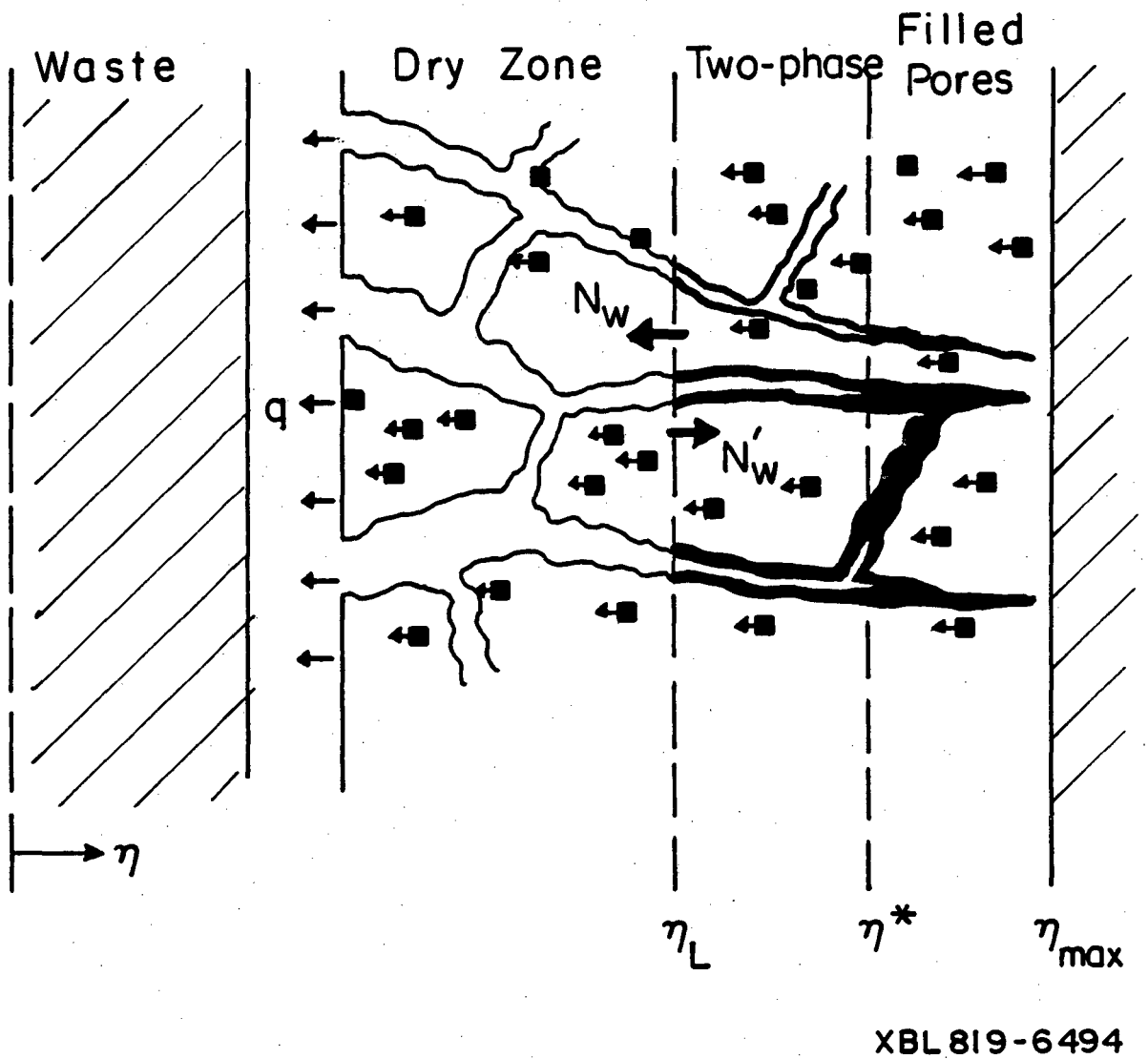
Waste
Dry Zone
Two-phase
Filled Pores
N_w
q
N'_w
η
η_L
η^*
η_{max}
XBL 819-6494

Figure 1.

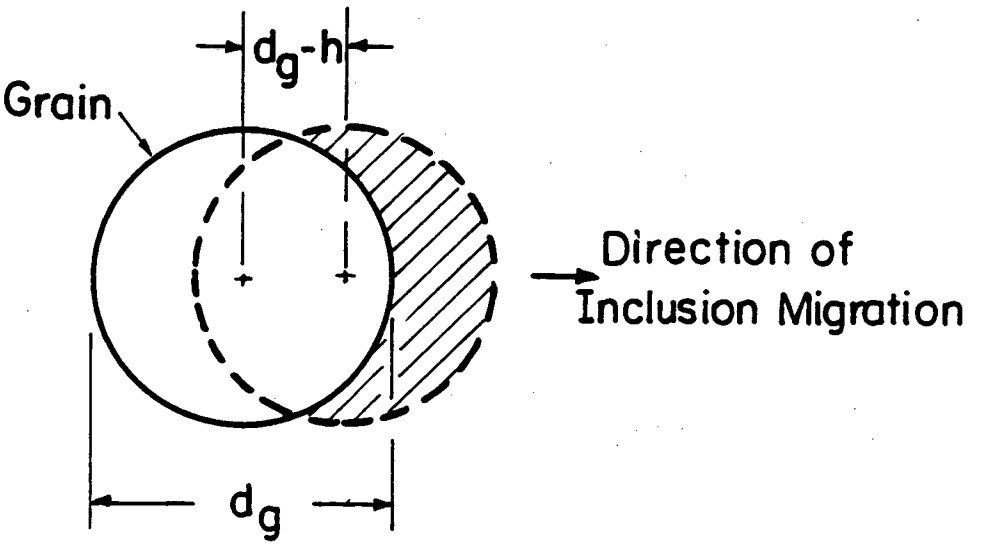

XBL819-6495

Figure 2.

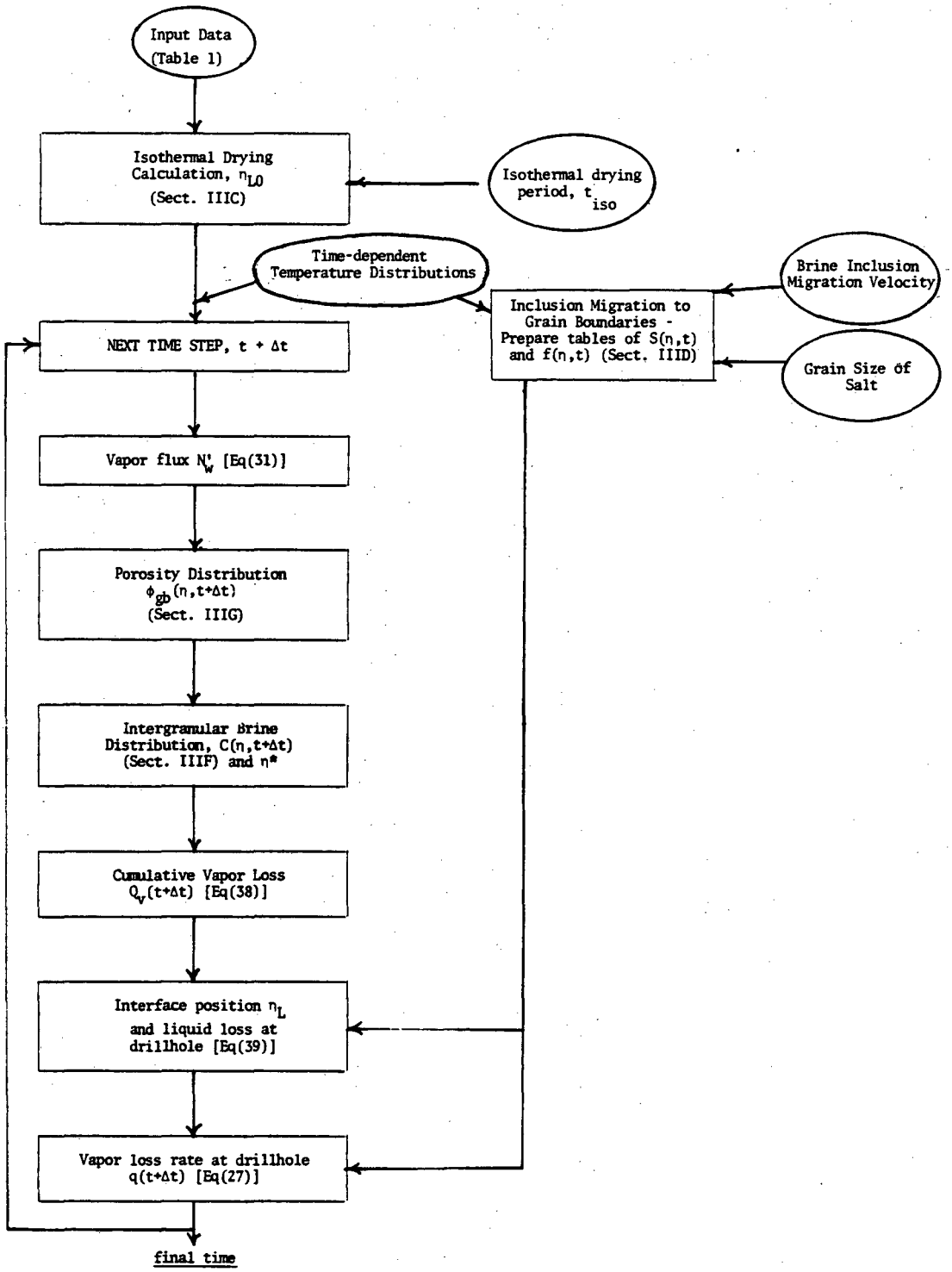

Figure 3.

--XBL 819-2031

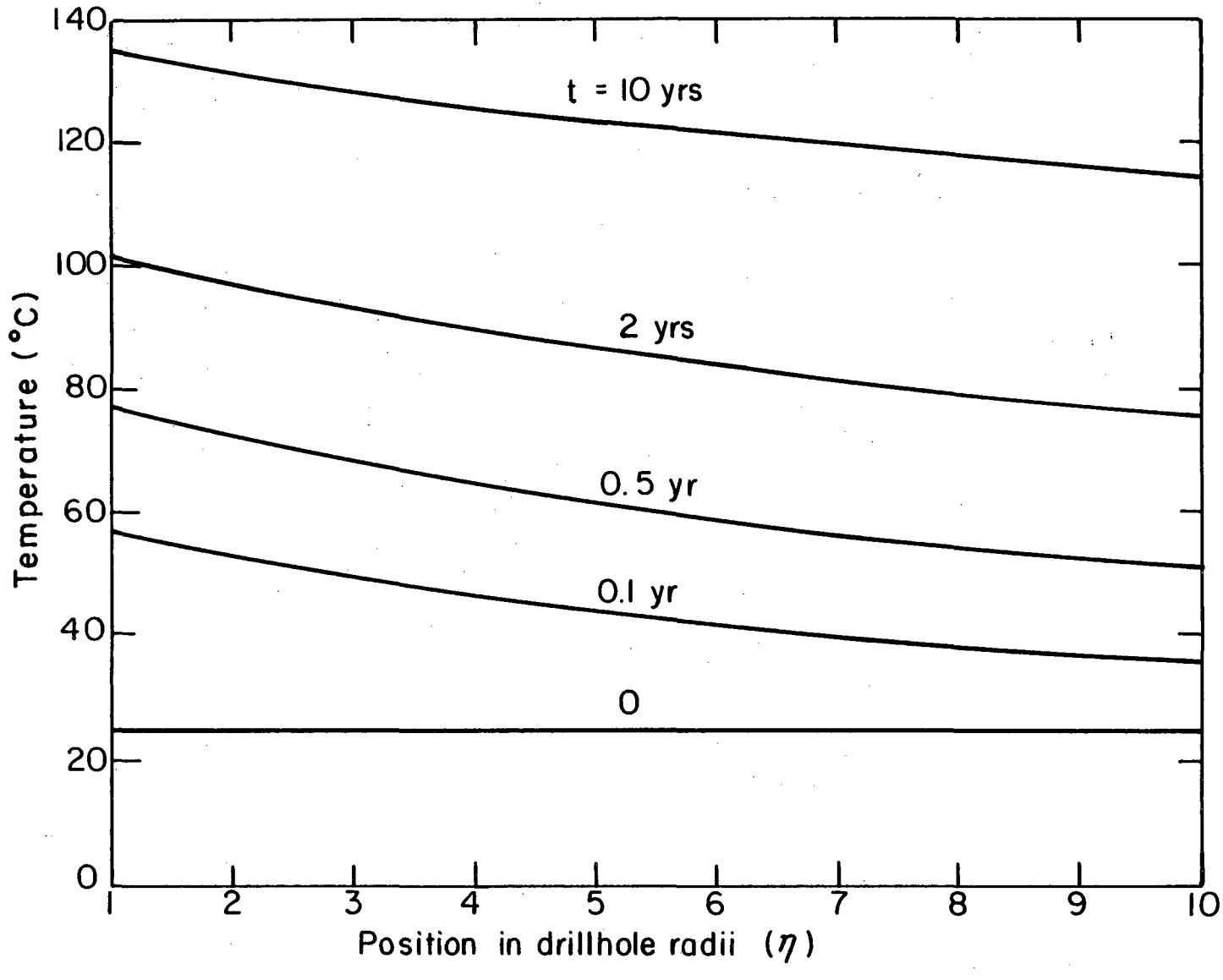

XBL 819-6497

Figure 4.

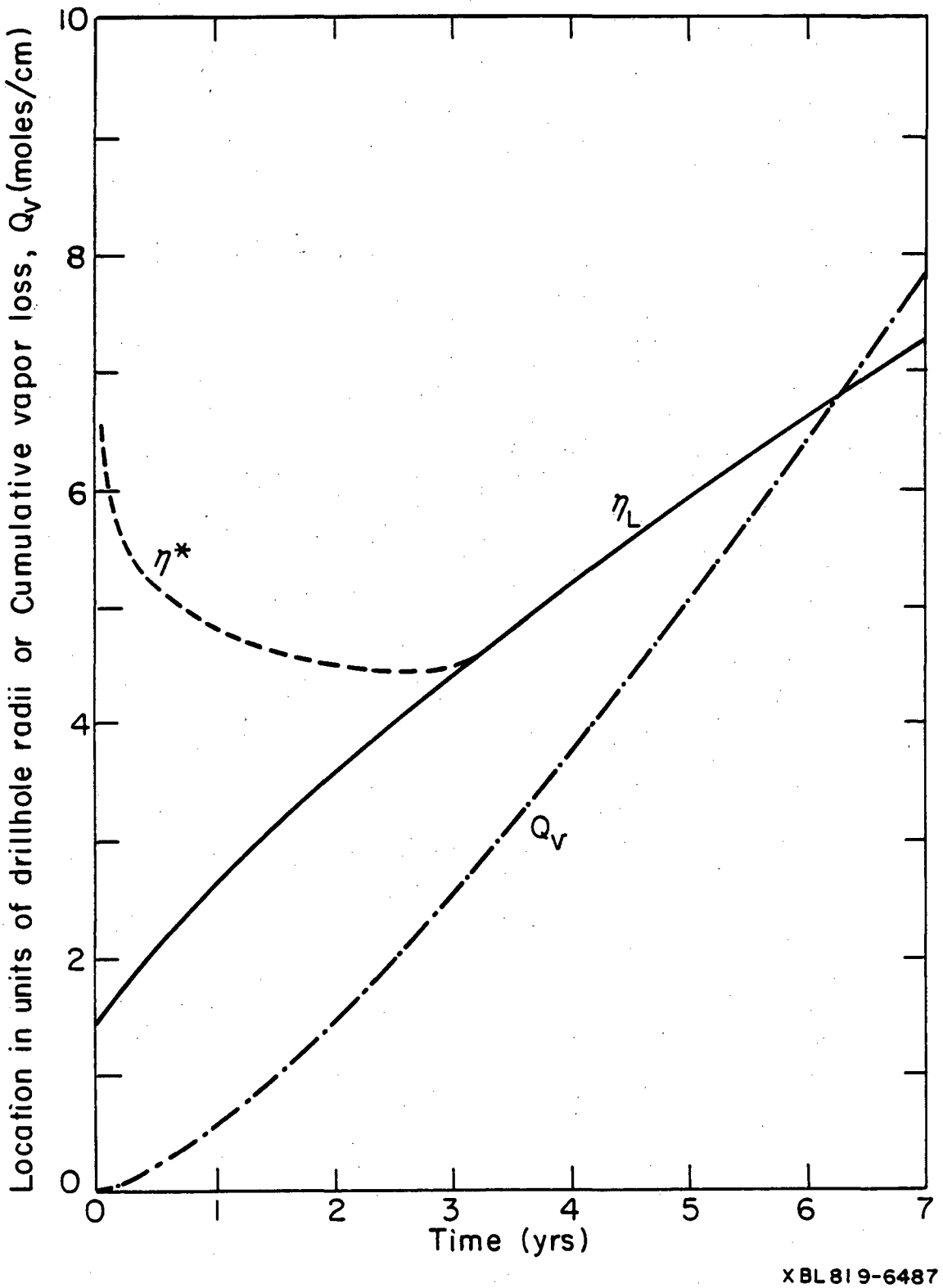
Location in units of drillhole radii or Cumulative vapor loss, Q_V (moles/cm)
10
8
6
4
2
0
0
1
2
3
4
5
6
7
Time (yrs)
η^*
η_L
Q_V
XBL819-6487

Figure 5.

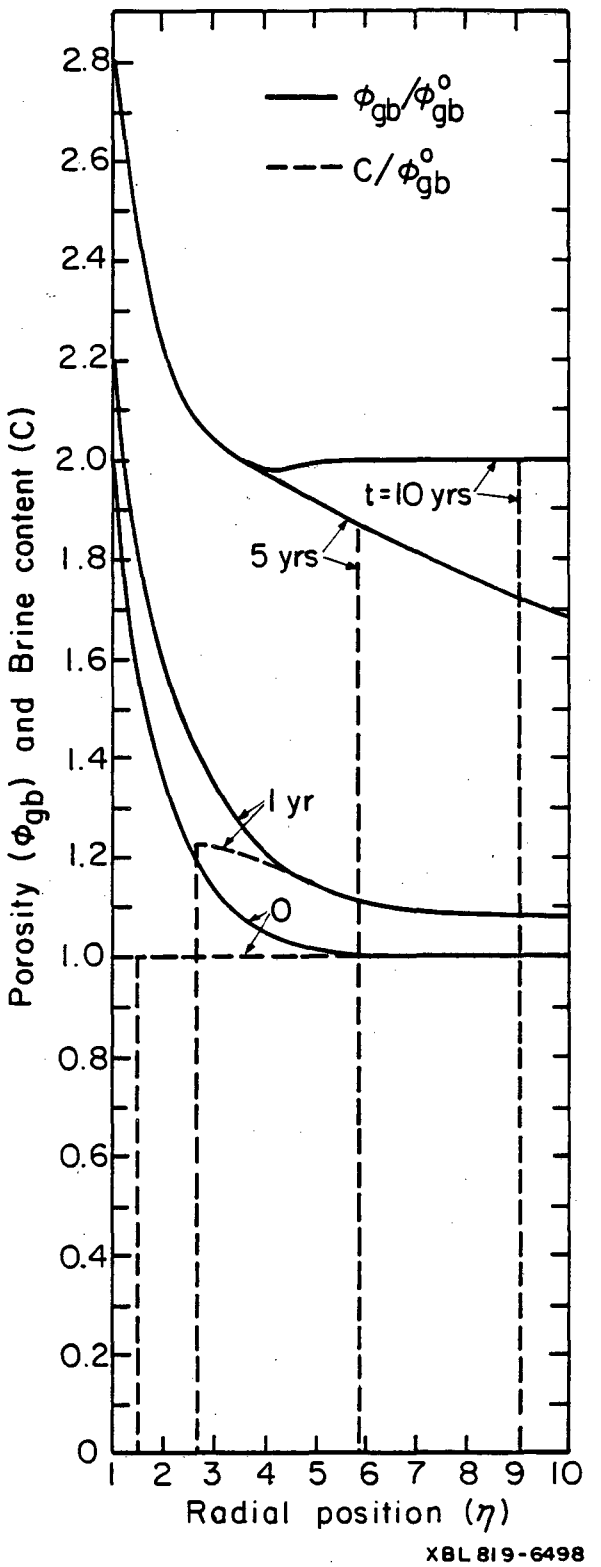
ϕ_{gb}/ϕ^o_{gb}
C/ϕ^o_{gb}
t=10 yrs
5 yrs
1 yr
0
Porosity (ϕ_{gb}) and Brine content (C)
Radial position (η)
2.8
2.6
2.4
2.2
2.0
1.8
1.6
1.4
1.2
1.0
0.8
0.6
0.4
0.2
0
1 2 3 4 5 6 7 8 9 10
XBL 819-6498

Figure 6.

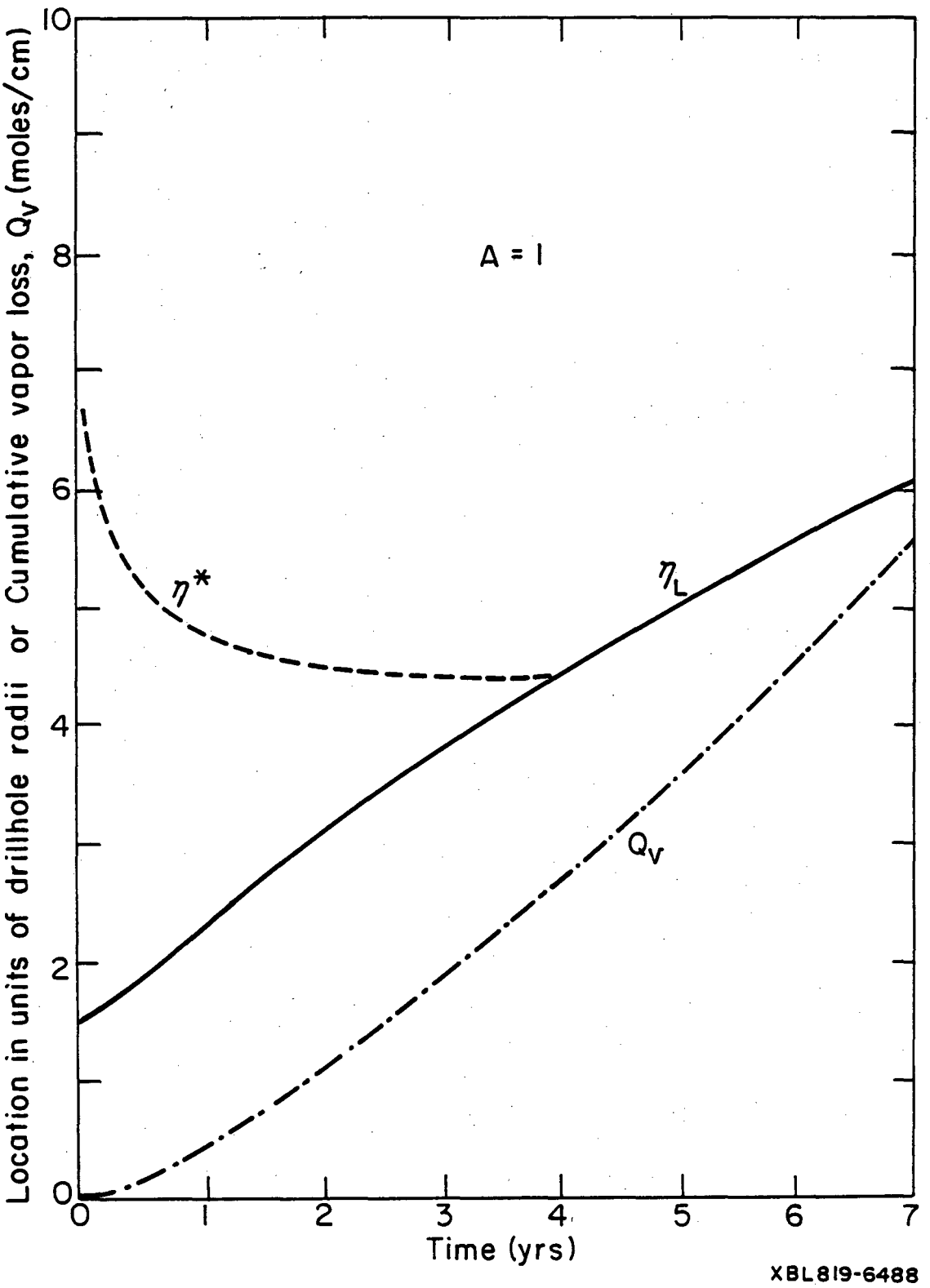
Location in units of drillhole radii or Cumulative vapor loss, Q_V (moles/cm)
10
8
6
4
2
0
A = 1
η^*
η_L
Q_V
0
1
2
3
4
5
6
7
Time (yrs)
XBL819-6488

Figure 7.

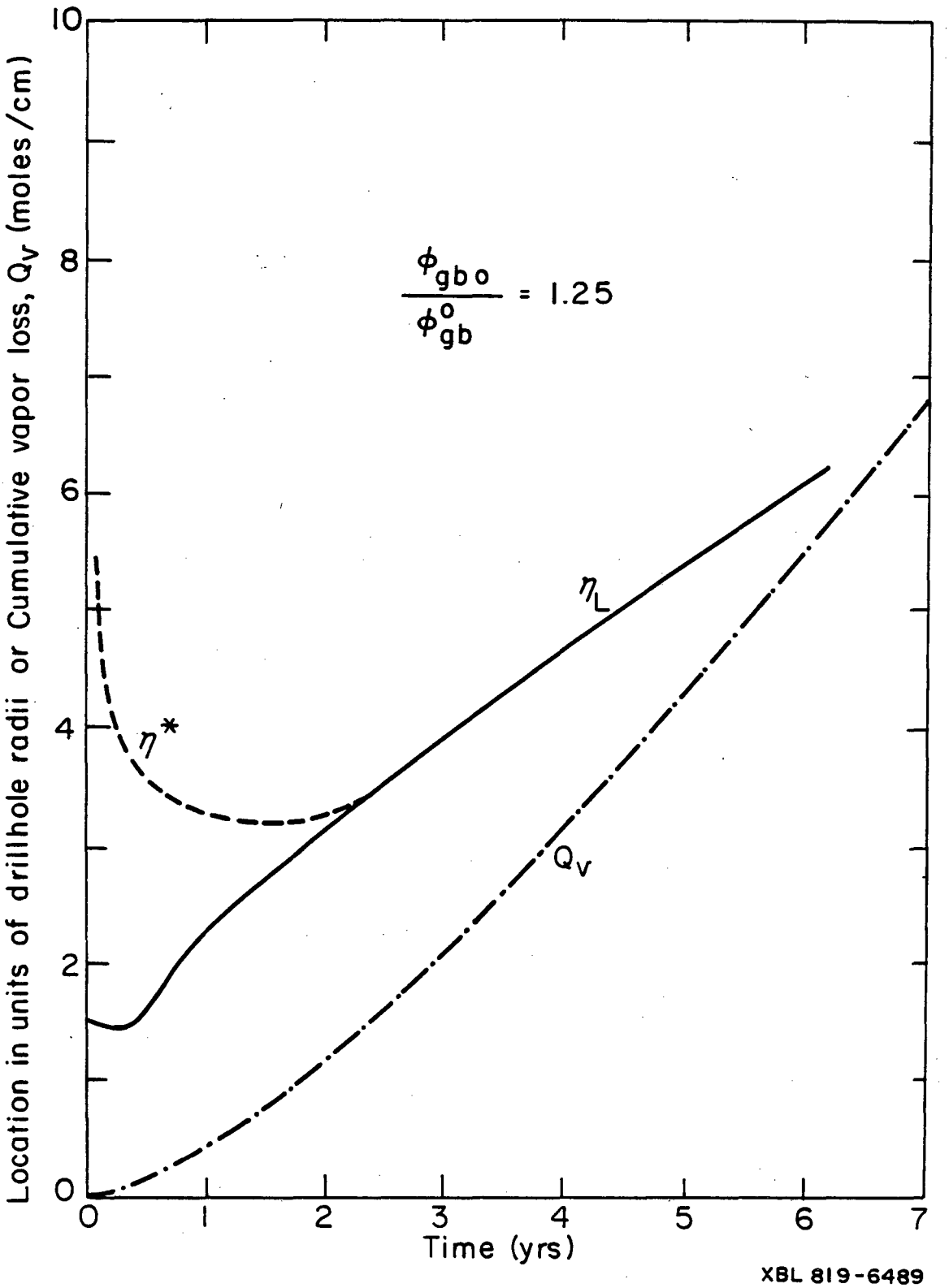
Location in units of drillhole radii or Cumulative vapor loss, Q_V (moles/cm)
10
8
6
4
2
0
0
1
2
3
4
5
6
7
Time (yrs)
$\frac{\phi_{gbo}}{\phi^o_{gb}} = 1.25$
η_L
η^*
Q_V
XBL 819-6489

Figure 8.

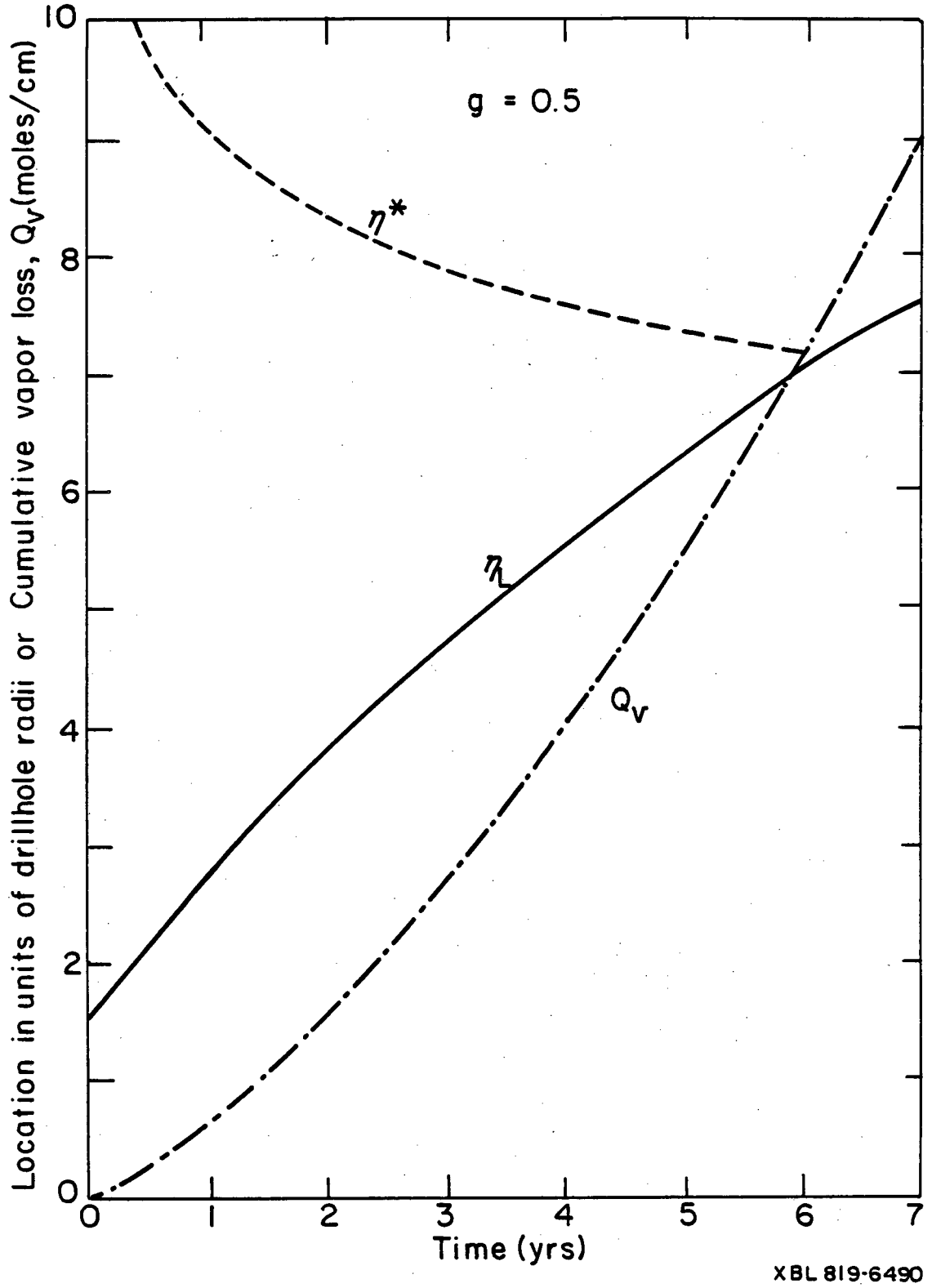
g = 0.5
η*
η
Q_v
Location in units of drillhole radii or Cumulative vapor loss, Q_v(moles/cm)
Time (yrs)
0
2
4
6
8
10
0
1
2
3
4
5
6
7
XBL 819-6490

Figure 9.

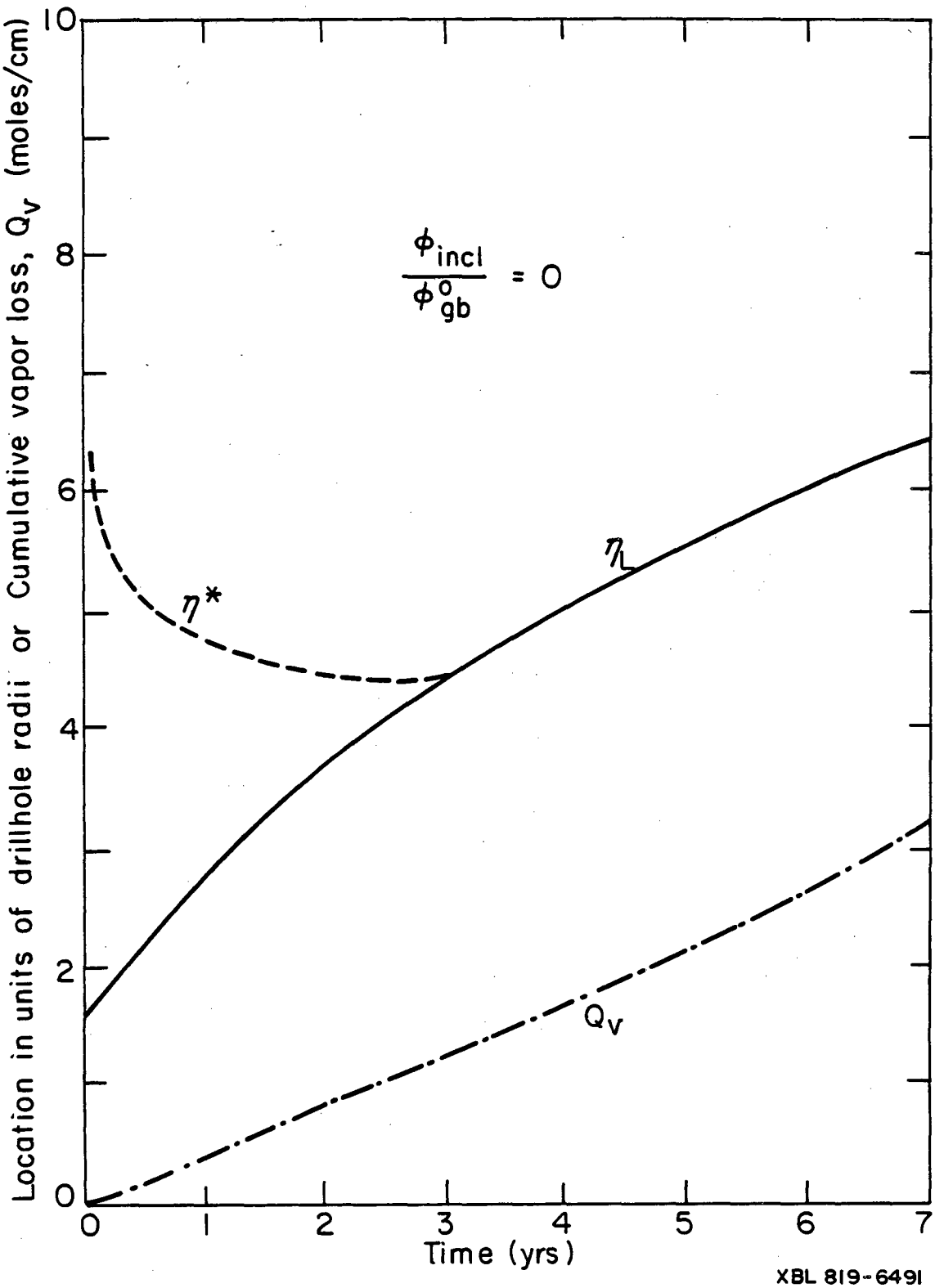
Location in units of drillhole radii or Cumulative vapor loss, Q_v (moles/cm)
10
8
6
4
2
0
$\frac{\phi_{incl}}{\phi^o_{gb}} = 0$
η^*
η_L
Q_v
0
1
2
3
4
5
6
7
Time (yrs)
XBL 819-6491

Figure 10.

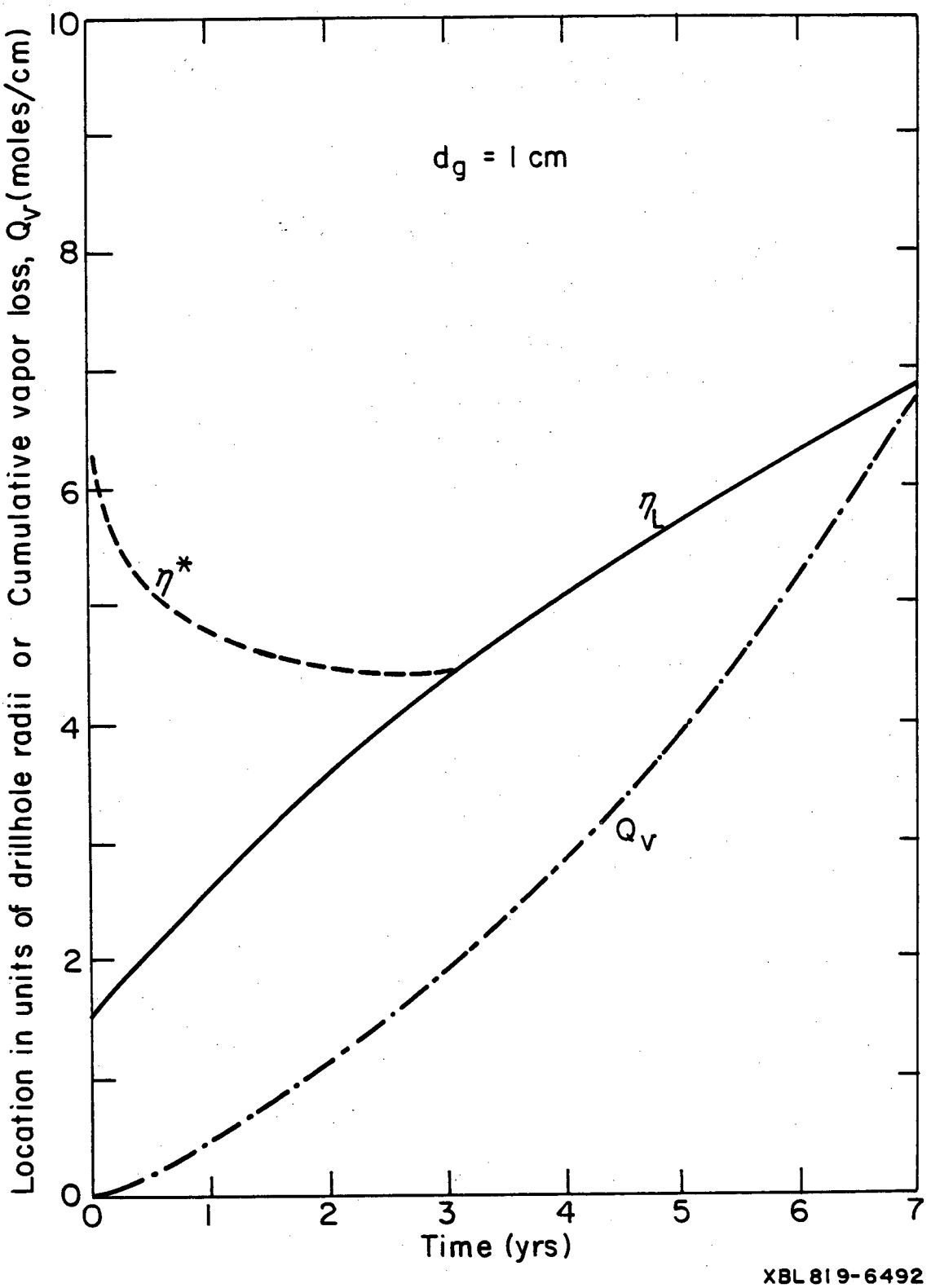
Location in units of drillhole radii or Cumulative vapor loss, Q_v (moles/cm)
10
8
6
4
2
0
d_g = 1 cm
η^*
η_L
Q_v
0
1
2
3
4
5
6
7
Time (yrs)
XBL 819-6492

Figure 11.

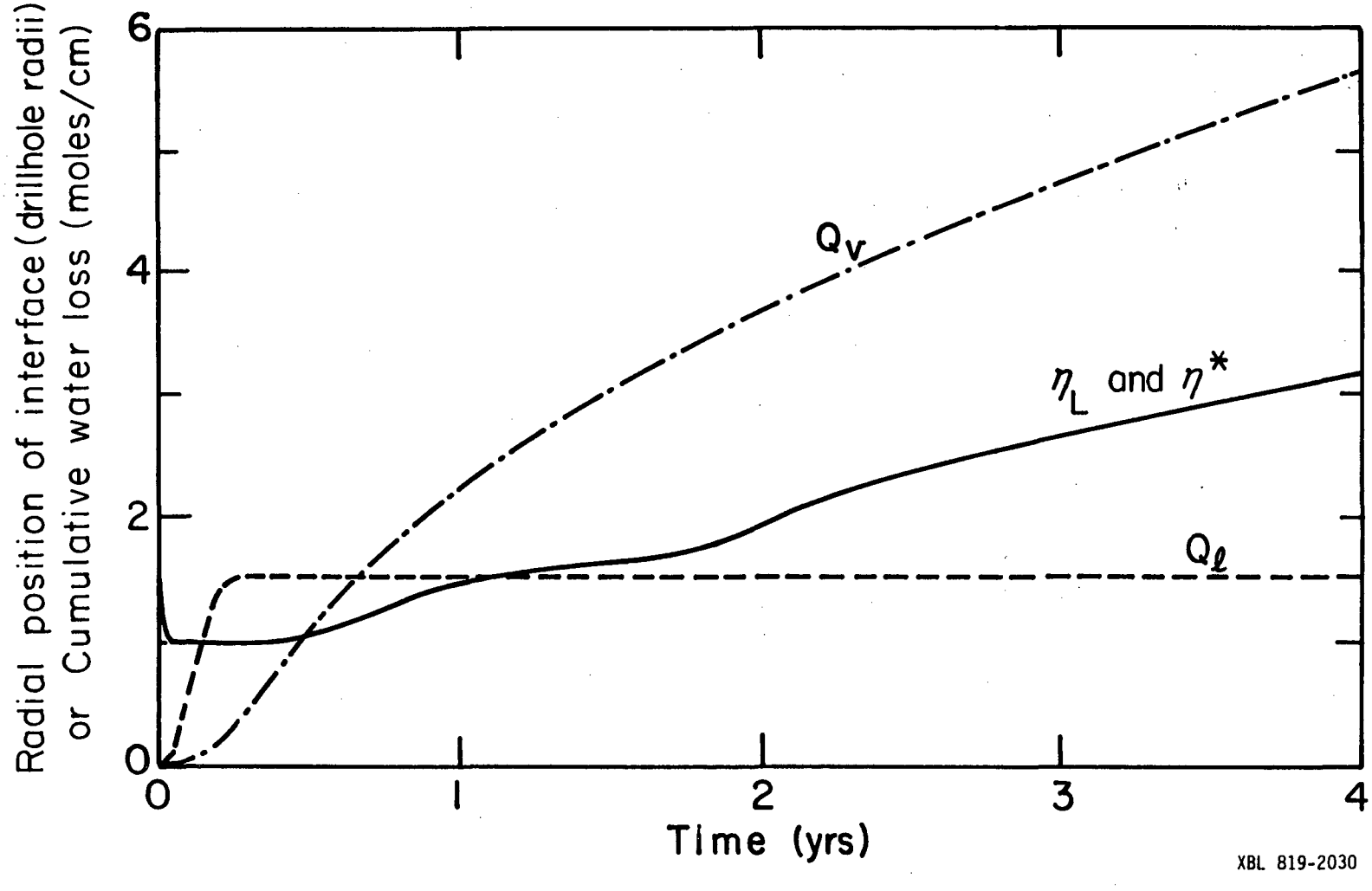
Radial position of interface (drillhole radii)
or Cumulative water loss (moles/cm)
6
4
2
0
0
1
2
3
4
Time (yrs)
Q_v
η_L and η^*
Q_ℓ
XBL 819-2030

Figure 12.

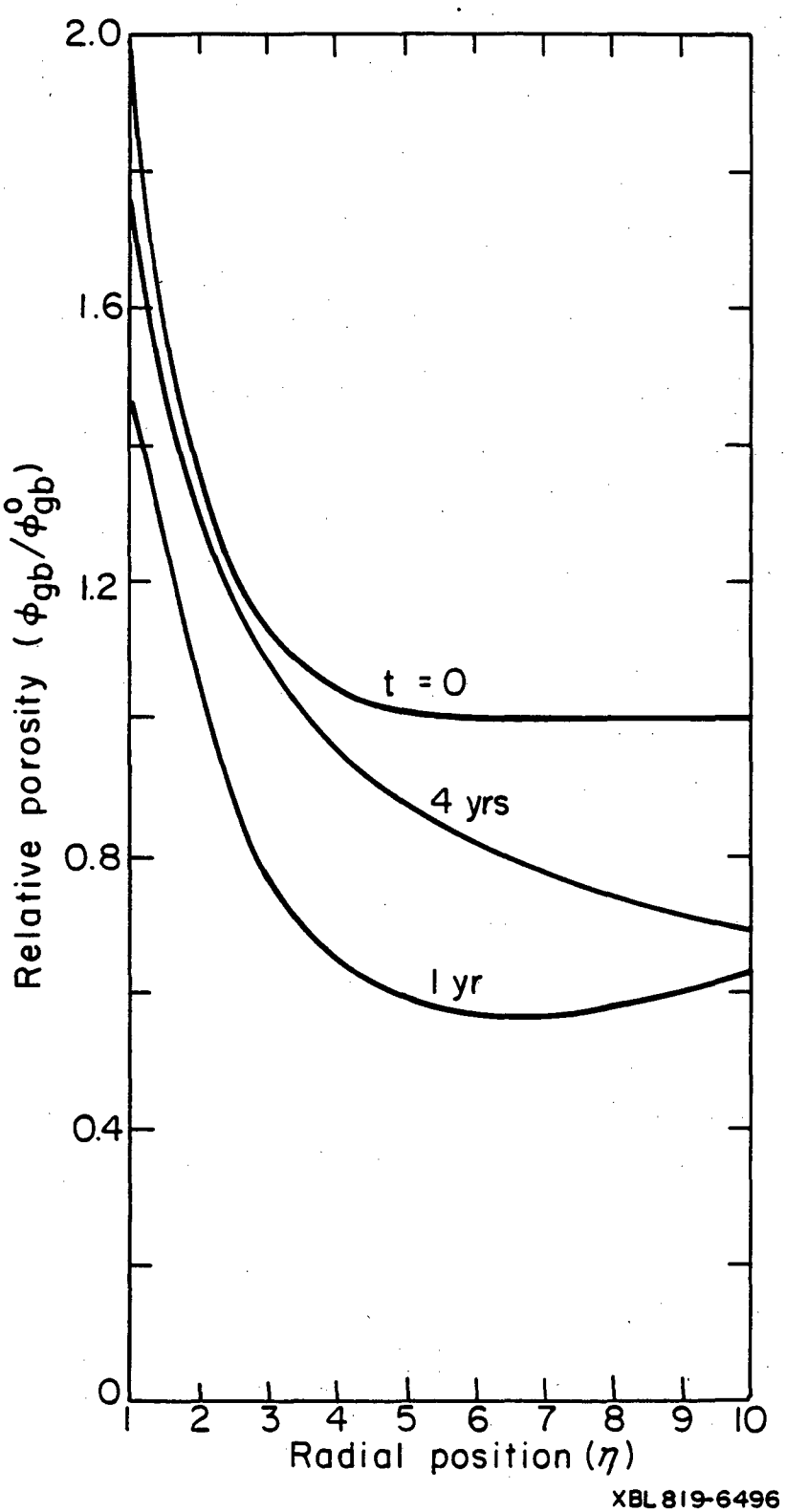
2.0
1.6
1.2
0.8
0.4
0
Relative porosity (ϕ_{gb}/ϕ^{o}_{gb})
t = 0
4 yrs
1 yr
1
2
3
4
5
6
7
8
9
10
Radial position (η)
XBL 819-6496

Figure 13.

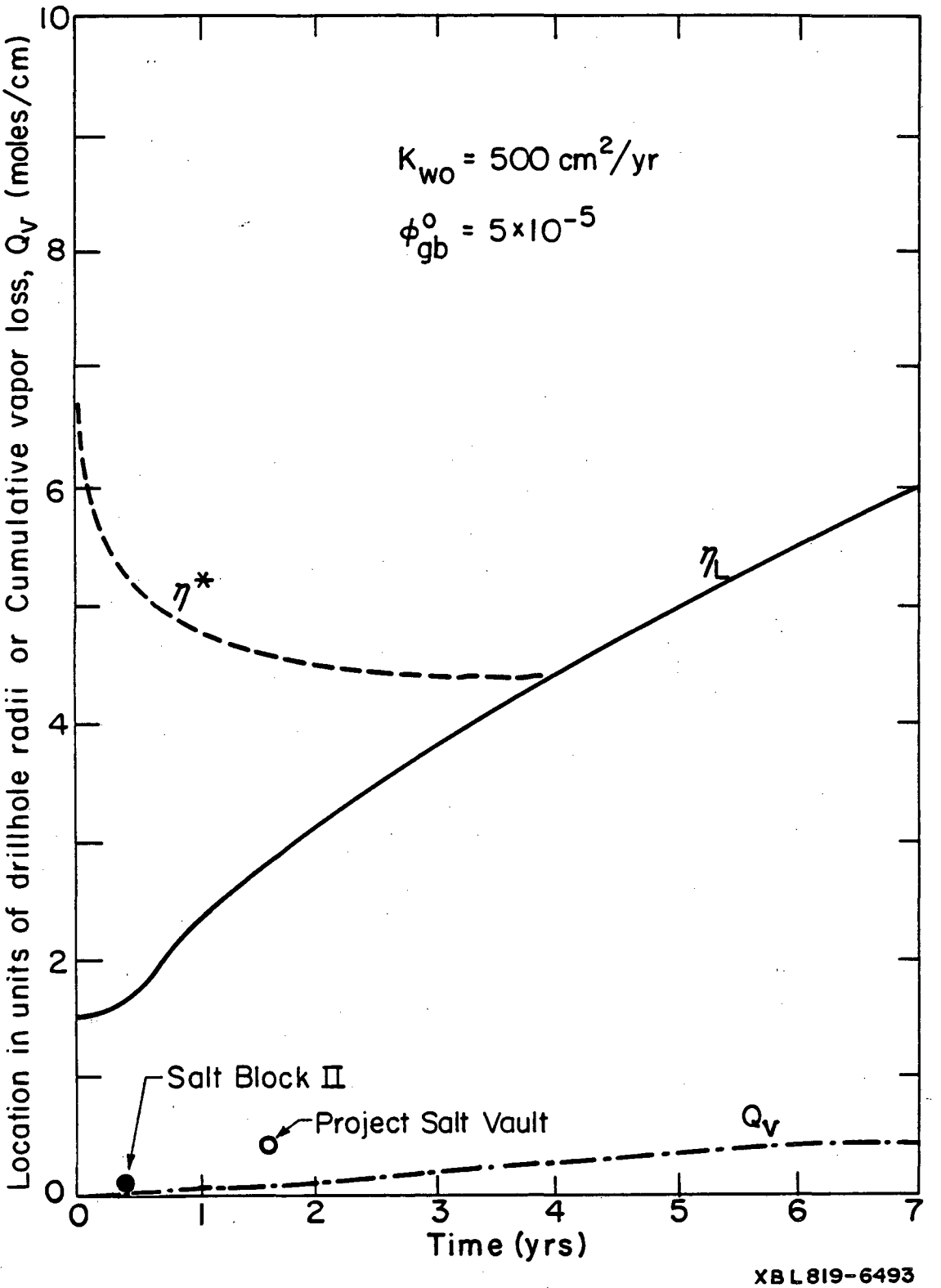
Location in units of drillhole radii or Cumulative vapor loss, Q_V (moles/cm)
10
8
6
4
2
0
K_{wo} = 500 cm^2/yr
ϕ^o_{gb} = 5×10^{-5}
η^*
η
Salt Block II
Project Salt Vault
Q_V
0
1
2
3
4
5
6
7
Time (yrs)
XBL819-6493

Figure 14.

Table 1 Inpurt Parameters for VAPMIG

Symbol	Units	Meaning	Numerical Value: Base Case	Numerical Value: Sensitivity Study
A	-	relative importance of Knudsen and bulk diffusion	0.01	1.0
R_o	cm	drillhole radius	30.5	30.5
ϕ^o_{gb}	-	initial volume fraction of brine on grain boundaries	$5x10^{-4}$	$5x10^{-5}$
ϕ_{incl}/ϕ^o_{gb}	-	relative amounts of brine in inclusions and on grain boundaries	1	0
ϕ_{gbo}/ϕ^o_{gb}	-	porosity at drillhole surface	2.0	1.25
g	-	measure of radial extent of porosity increase due to drillhole boring	1.0	0.5
p_{ao}	bar	air pressure in drillhole	1.0	1.0
p_{wo}	bar	water vapor pressure in drillhole	0.0	0.0
K_{wo}	cm^2/yr	initial Knudsen diffusivity of salt at drillhole surface	$1x10^4$	500
ρ_w	$moles/cm^3$	water concentration of saturated brine	0.05	0.05
d_g	cm	grain diameter	0.5	1.0
α_s	$°C^{-1}$	volumetric thermal expansion coefficient of solid salt	$1.2x10^{-4}$	$1.2x10^{-4}$
F	-	fraction of solid thermal expansion accommodated by porosity	0	0.5
α_B	$°C^{-1}$	volumetric thermal expansion coefficient of brine	$4.6x10^{-4}$	$4.6x10^{-4}$
p_w^{sat}	bar	vapor pressure of water over saturated brine	from ONWI 208	
V	cm/yr	inclusion migration velocity	Jenks correlations (Ref. 1)	

This report was done with support from the Department of Energy. Any conclusions or opinions expressed in this report represent solely those of the author(s) and not necessarily those of The Regents of the University of California, the Lawrence Berkeley Laboratory or the Department of Energy.

Reference to a company or product name does not imply approval or recommendation of the product by the University of California or the U.S. Department of Energy to the exclusion of others that may be suitable.

TECHNICAL INFORMATION DEPARTMENT
LAWRENCE BERKELEY LABORATORY
UNIVERSITY OF CALIFORNIA
BERKELEY, CALIFORNIA 94720